

Vascular Endothelial Growth Factor-Angiopoietin Chimera With Improved Properties for Therapeutic Angiogenesis

Andrey Anisimov, Denis Tvorogov, Annamari Alitalo, Veli-Matti Leppänen, Yuri An, Eun Chun Han, Fabrizio Orsenigo, Emilia Ilona Gaál, Tanja Holopainen, Young Jun Koh, Tuomas Tammela, Petra Korpisalo, Salla Keskitalo, Michael Jeltsch, Seppo Ylä-Herttuala, Elisabetta Dejana, Gou Young Koh, Chulhee Choi, Pipsa Saharinen and Kari Alitalo

Circulation. 2013;127:424-434

doi: 10.1161/CIRCULATIONAHA.112.127472

Circulation is published by the American Heart Association, 7272 Greenville Avenue, Dallas, TX 75231

Copyright © 2013 American Heart Association, Inc. All rights reserved.

Print ISSN: 0009-7322. Online ISSN: 1524-4539

The online version of this article, along with updated information and services, is located on the World Wide Web at:

<http://circ.ahajournals.org/content/127/4/424>

Data Supplement (unedited) at:

<http://circ.ahajournals.org/content/suppl/2013/01/25/127.4.424.DC1.html>

Permissions: Requests for permissions to reproduce figures, tables, or portions of articles originally published in *Circulation* can be obtained via RightsLink, a service of the Copyright Clearance Center, not the Editorial Office. Once the online version of the published article for which permission is being requested is located, click Request Permissions in the middle column of the Web page under Services. Further information about this process is available in the [Permissions and Rights Question and Answer](#) document.

Reprints: Information about reprints can be found online at:

<http://www.lww.com/reprints>

Subscriptions: Information about subscribing to *Circulation* is online at:

<http://circ.ahajournals.org/subscriptions/>

Vascular Endothelial Growth Factor–Angiopoietin Chimera With Improved Properties for Therapeutic Angiogenesis

Andrey Anisimov, PhD; Denis Tvorogov, PhD; Annamari Alitalo, DVM;
Veli-Matti Leppänen, PhD; Yuri An, MSc; Eun Chun Han, MD; Fabrizio Orsenigo, MSc;
Emília Ilona Gaál, MD; Tanja Holopainen, MD; Young Jun Koh, PhD; Tuomas Tammela, MD, PhD;
Petra Korpisalo, MD; Salla Keskitalo, MSc; Michael Jeltsch, PhD; Seppo Ylä-Herttuala, MD, PhD;
Elisabetta Dejana, PhD; Gou Young Koh, MD, PhD; Chulhee Choi, MD, PhD;
Pipsa Saharinen, PhD; Kari Alitalo, MD, PhD

Background—There is an unmet need for proangiogenic therapeutic molecules for the treatment of tissue ischemia in cardiovascular diseases. However, major inducers of angiogenesis such as vascular endothelial growth factor (VEGF/VEGF-A) have side effects that limit their therapeutic utility in vivo, especially at high concentrations. Angiopoietin-1 has been considered to be a blood vessel stabilization factor that can inhibit the intrinsic property of VEGF to promote vessel leakiness. In this study, we have designed and tested the angiogenic properties of chimeric molecules consisting of receptor-binding parts of VEGF and angiopoietin-1. We aimed at combining the activities of both factors into 1 molecule for easy delivery and expression in target tissues.

Methods and Results—The VEGF–angiopoietin-1 (VA1) chimeric protein bound to both VEGF receptor-2 and Tie2 and induced the activation of both receptors. Detailed analysis of VA1 versus VEGF revealed differences in the kinetics of VEGF receptor-2 activation and endocytosis, downstream kinase activation, and VE-cadherin internalization. The delivery of a VA1 transgene into mouse skeletal muscle led to increased blood flow and enhanced angiogenesis. VA1 was also very efficient in rescuing ischemic limb perfusion. However, VA1 induced less plasma protein leakage and myeloid inflammatory cell recruitment than VEGF. Furthermore, angioma-like structures associated with VEGF expression were not observed with VA1.

Conclusions—The VEGF–angiopoietin-1 chimera is a potent angiogenic factor that triggers a novel mode of VEGF receptor-2 activation, promoting less vessel leakiness, less tissue inflammation, and better perfusion in ischemic muscle than VEGF. These properties of VA1 make it an attractive therapeutic tool. (*Circulation*. 2013;127:424-434.)

Key Words: angiogenesis inducers ■ capillary permeability ■ gene therapy ■ ischemia ■ vascular endothelium

Angiogenesis, the process of the formation of new blood vessels from preexisting ones, occurs in all vascularized organs during embryogenesis. In adults, angiogenesis is observed mainly in a variety of pathological conditions such as wound healing, tumor growth, and proliferative retinal vasculopathies.^{1,2} Members of the vascular endothelial growth factor (VEGF) family, including VEGF-A, -B, -C, and -D and placenta growth factor, play major roles in various forms of angiogenesis.³ There is a great need in the clinic for proangiogenic therapeutic molecules that can induce angiogenesis in patients suffering from tissue ischemia.⁴

Currently used angiogenic inducers rely mainly on stimulation of the VEGF receptor-2 (VEGFR-2) signal transduction pathway in endothelial cells.

Clinical Perspective on p 434

VEGF-A (VEGF hereafter), the strongest inducer of angiogenesis, has serious side effects, including an increased vessel permeability or leakiness, leading to tissue swelling, fibrin deposition, and tissue inflammation.⁵ VEGF-E, another family member that is encoded by the Orf virus, potently stimulates

Received June 27, 2012; accepted December 4, 2012.

From the Wihuri Research Institute, Helsinki, Finland (A. Anisimov, V.-M.L., P.S., K.A.); Molecular/Cancer Biology Program, Biomedicum Helsinki and Helsinki University Central Hospital, University of Helsinki, Helsinki, Finland (A. Anisimov, D.T., V.-M.L., E.I.G., T.H., T.T., S.K., M.J., P.S., K.A.); Department of Biotechnology and Molecular Medicine, A.I. Virtanen Institute for Molecular Sciences, University of Eastern Finland, Kuopio, Finland (A. Alitalo, P.K., S.Y.-H.); National Research Laboratory of Vascular Biology and Stem Cells (Y.J.K., G.Y.K.), Department of Bio and Brain Engineering (Y.A., E.C.H., C.C.), and Graduate School of Medical Science and Engineering (E.C.H., C.C.), Korea Advanced Institute of Science and Technology, Daejeon, Korea; IFOM, FIRC Institute of Molecular Oncology Foundation, Milan, Italy (F.O., E.D.); Università di Milano, School of Sciences, Milan, Italy (E.D.); and Department of Neurosurgery, Helsinki University Central Hospital, Helsinki, Finland (E.I.G.). Dr A. Alitalo is now at the Swiss Federal Institute of Technology, Basel, Switzerland.

The online-only Data Supplement is available with this article at <http://circ.ahajournals.org/lookup/suppl/doi:10.1161/CIRCULATIONAHA.112.127472/-/DC1>.

Correspondence to Kari Alitalo, MD, PhD, Wihuri Research Institute, Biomedicum Helsinki, PO Box 63 (Haartmaninkatu 8), University of Helsinki, Helsinki, 00014 Finland. E-mail Kari.Alitalo@Helsinki.fi

© 2013 American Heart Association, Inc.

Circulation is available at <http://circ.ahajournals.org>

DOI: 10.1161/CIRCULATIONAHA.112.127472

angiogenesis but promotes somewhat less inflammation and vascular hyperpermeability than VEGF.⁶ However, VEGF-E is potentially immunogenic because of its virus-derived epitopes; the same concern applies to molecules comprising parts of VEGF-E and placenta growth factor.⁷ VEGF-B hardly stimulates new vessel formation in skeletal muscle, but recent studies have shown that its high or prolonged overexpression leads to an impressive expansion of the coronary vasculature.⁸ Recent studies have also indicated that the lymphangiogenic growth factors VEGF-C and VEGF-D induce functional blood and lymphatic vessels in mouse and rabbit skeletal muscle, but this effect was accompanied by infiltration of inflammatory cells.^{9,10} A chimeric protein comprising the receptor-binding VEGF homology domain of VEGF, flanked by VEGF-C–derived N- and C-terminal propeptides,¹¹ induced less vessel permeability but retained the property of inflammatory cell recruitment.¹⁰ Interestingly, 1 of the 2 naturally occurring VEGF-D isoforms, generated by alternative proteolysis (D_{100–195}), was recently shown to be a specific VEGFR-2 ligand that was weakly angiogenic without evidence of lymphangiogenic activity.¹² Thus, the search is still ongoing for efficient vascular growth factors without permeability and inflammatory properties.

Angiopoietin-1 (Ang1) signaling has been shown to mediate vessel stabilization and to inhibit vascular leak induced by a variety of stimuli.¹³ Ang1 also inhibited VEGF-induced leukocyte adhesion to endothelial cells.¹⁴ Coexpression of VEGF and Ang1 in the skin of transgenic mice resulted in the generation of larger, leakage-resistant vessels.¹⁵ In subsequent studies, attempts were made to overexpress Ang1 with VEGF in a therapeutic setting, delivered via the same or separate viral vectors.^{16,17} In these studies, Ang1 was shown to recruit pericytes and smooth muscle cells, facilitating the formation of more mature vessels, which were less leaky for plasma proteins.

To combine the desired growth factor properties into a single protein, we have designed a chimeric molecule by fusing the receptor-binding parts of human VEGF and Ang1. We show that the angiogenic activity of this molecule is similar to that of VEGF, but it induces many fewer vessel abnormalities and much less leakiness and tissue inflammation than VEGF.

Methods

Tissue Transduction With the Recombinant Adeno-Associated Viral Vectors

Six- to 7-week-old female FVB/N mice were anesthetized with xylazine (Rompun Vet; Bayer Healthcare, Leverkusen, Germany) and ketamine (Ketalar; Pfizer, New York, NY), and 3×10^{10} recombinant adeno-associated viral (rAAV) particles (in 30- μ L volume) were injected into each tibialis anterior muscle. All mouse experiments were approved by the Provincial State Office of Southern Finland and were carried out in accordance with institutional guidelines.

Immunohistochemistry of Skeletal Muscle Samples

The tibialis anterior muscles were isolated and frozen in OCT (optimal cutting temperature). Cryosections (10 μ m) were cut, fixed in acetone, and immunostained with rat anti-platelet endothelial cell adhesion molecule-1 (BD Biosciences), rat anti-CD45 (BD Biosciences), rat F4/80 (AbD Serotec; MorphoSys AG), mouse anti-smooth muscle actin-Cy3 (Sigma-Aldrich), rat anti-mouse NG2, or goat anti-mouse platelet-derived growth factor receptor- β (R&D Systems). Hoechst 33258 was used for DNA staining. The microvessel area density was quantified with ImageJ software (National Institutes of Health).

Results are presented as mean \pm SD. The samples were analyzed with either an Axioplan 2 microscope (Carl Zeiss AG; objectives, $\times 10$ numerical aperture (NA)=0.3 working distance (WD) 5.6 mm and $\times 20$ NA=0.5 and WD 2.0 mm; camera, Zeiss AxioCamHRm 14-bit grayscale charge-coupled device; acquisition software, Zeiss AxioVision 4.6) or an LSM 510 Meta confocal microscope equipped with a digital camera (Carl Zeiss AG; objective, $\times 10$ Fluor 0.50, Differential Interference Contrast (DIC); acquisition software, LSM release 3.2).

Fluorescent Angiography of Blood Vessels via Cardiac Perfusion

Blood vessels were directly visualized by cardiac perfusion with the lipophilic carbocyanine dye 1,1'-dioctadecyl-3,3',3'-tetramethylindocarbocyanine perchlorate (DiI) as described previously.¹⁰ After perfusion, the tibialis anterior muscle was isolated, and 120- μ m sections were analyzed by confocal microscopy using an excitation wavelength of 543 nm.

Miles Assay in Skeletal Muscle

rAAVs encoding VA1, VEGF, Ang1, Ang2, or human serum albumin were expressed for 2 weeks in the tibialis anterior muscles of 2-month-old FVB/N female mice. The mice were anesthetized, and 300 μ L of 1% Evans Blue (in PBS) was injected into the tail vein. The dye was allowed to circulate for 30 to 45 minutes, followed by cardiac perfusion with PBS (10 mL per mouse). Tibialis anterior muscles were isolated and weighed, and the dye was extracted overnight with deionized formamide (1 mL per muscle) and measured at an optical density of 620 nm.

In Vivo Signal Transduction Studies

FVB/N mice were injected intravenously via the tail vein with pure proteins at the doses indicated in the figure legends and in the text. Mice were euthanized by cervical dislocation after various periods of time (10, 30, or 60 minutes). Lungs were flash-frozen in liquid nitrogen and stored until use. Tissue samples were homogenized in lysis buffer (0.5% Triton X-100/0.5% NP-40 in PBS supplemented with protease and phosphatase inhibitors using PowerLyzer 24 Bench Top Bead-Based Homogenizer, MO BIO Laboratories, Inc); insoluble material was removed by centrifugation in a bench-top centrifuge (200 00g at 4°C for 5 minutes); and protein concentration was determined by the Bradford method. Soluble protein (200 μ g) was resolved in 4% to 20% SDS-PAGE, transferred onto polyvinylidene difluoride membrane, and Western blotted with the indicated antibodies.

Statistical Analysis

If equal variances were assumed, we evaluated statistical significance by 1-way ANOVA followed by the Dunnett (2-sided) post hoc test, with values of $P < 0.05$ regarded as significant. When pairwise comparisons between experimental groups were made, the Tukey test was used. If the variances were not equal, the Games-Howell test was used as a post hoc test, with values of $P < 0.05$ regarded as significant. When appropriate, an unpaired t test was also used. The results are presented as mean \pm SD unless indicated otherwise.

An expanded Materials and Methods section containing detailed descriptions of the construction, production, and testing of the rAAV vectors; cell survival assay using methylthiazolyl-diphenyl-tetrazolium bromide (MTT, Sigma-Aldrich); protein expression and purification; quantification of growth factor expression in transduced skeletal muscle by ELISA; immunocytochemistry; biotinylation and ubiquitinylation experiments; immunohistochemistry; Doppler ultrasound measurement of blood perfusion; and hind-limb ischemia models is provided in the online-only Data Supplement.

Results

Production and Receptor-Binding Properties of VEGF-Ang1 Chimeric Proteins

The schematic structures of the VEGF and Ang1 subunit polypeptide chains and of the VEGF-Ang1 chimera are shown in Figure 1A.¹⁸ Mature VEGF is an antiparallel homodimer

stabilized by disulfide bonds,¹⁹ whereas Ang1 (and COMP-Ang1)²⁰ forms higher-order multimers. The receptor-binding regions of VEGF and Ang1, which reside in the VEGF homology domain and fibrinogen-like domain, respectively, were fused in the same orientation with or without the Ang1 linker domain that accommodates the pericellular matrix-binding portion of Ang1²¹ (constructs designated VA1 and VA2 in Figure 1A). The proteins were produced in plasmid-transfected 293T cells and in Sf21 insect cells, and their receptor-binding properties were tested. Unlike native VEGF and Ang1, which bound only to their cognate receptors VEGFR-1/VEGFR-2 and Tie2, respectively, both VA polypeptides bound to all 3 receptors (Figure 1B). The binding affinity of VA1 to its cognate receptors

was determined by the use of isothermal titration calorimetry (Figure 1C). Analysis of the VA1 protein by gel electrophoresis in reducing versus nonreducing conditions demonstrated that, similar to VEGF but unlike Ang1, the majority of the mature VA1 protein formed disulfide-bonded dimers, although a minor portion of the protein produced in mammalian 293T cells appeared as high-order multimers (Figure 1D and Figure 1A in the online-only Data Supplement).

We next analyzed whether the VA1 protein can simultaneously bind to both VEGFR-2 and Tie2. Purified VEGFR-2-Fc protein,²² bound to protein G Sepharose, was incubated with VA1-containing medium from transfected cells. After several washes, the beads were incubated with lysates of human

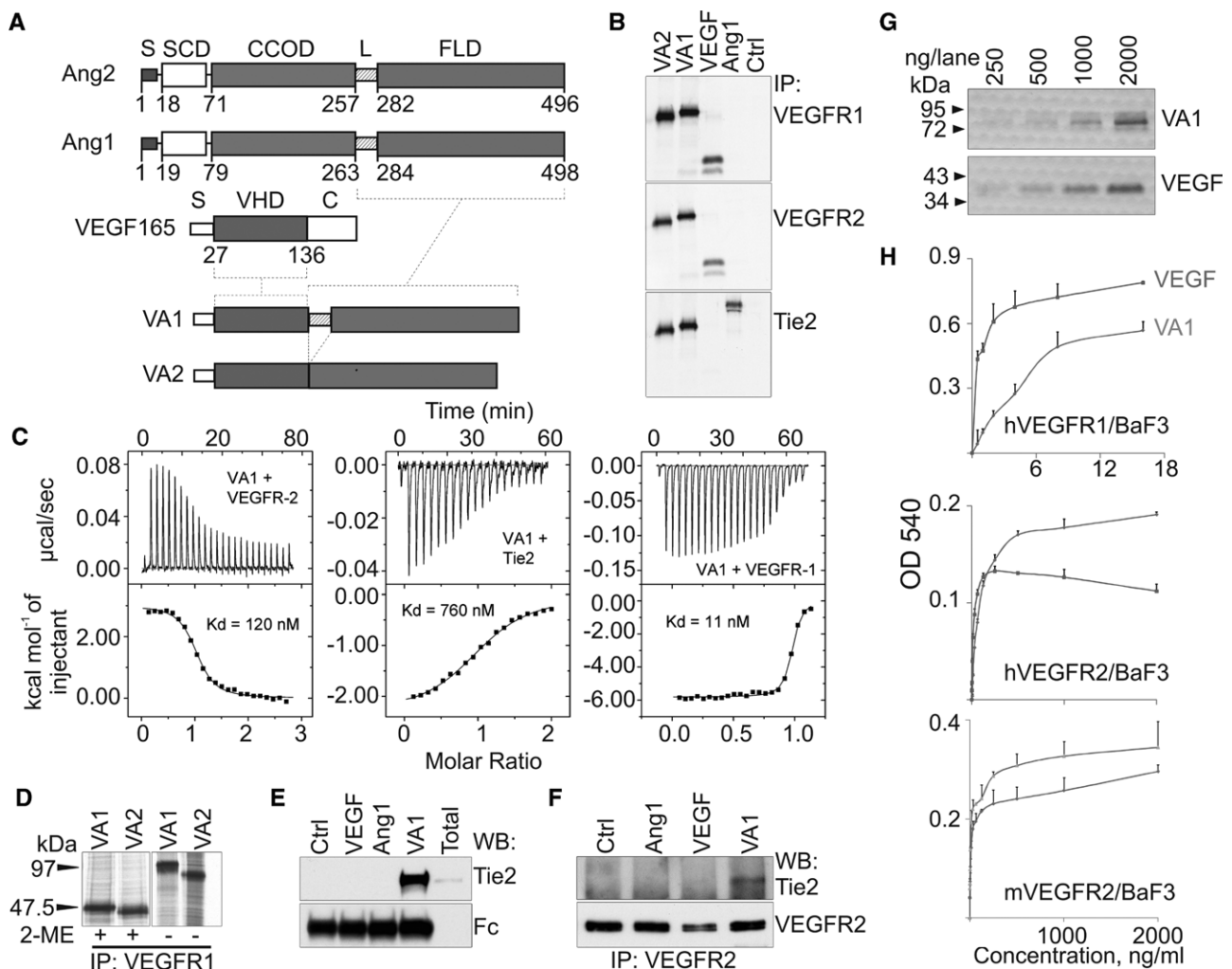


Figure 1. Design and receptor-binding analysis of the ligands used in the study. **A**, Schematic (domain) view of angiopoietin (Ang)-1, Ang2, vascular endothelial growth factor (VEGF)-165, and VA1 and VA2 proteins. Domain boundaries (amino acid numbers as designated in Kim et al¹⁸) are shown. The number of amino acid residue indicates the length of the VEGF homology domain (VHD) domain. C indicates C-terminal part of VEGF165; CCOD, coiled-coil oligomeric domain; FLD, fibrinogen-like domain; L, linker region of Ang1; S, signal peptide; and SCD, superclustering domain. **B**, Immunoprecipitation (IP) of [³⁵S]-labeled growth factors from media of 293T cells transfected with the indicated recombinant adeno-associated viral (rAAV) vectors. **C**, Thermodynamic analysis of VA1 binding to VEGFR-2, Tie-2, and VEGFR-1. Binding affinities (K_ds) are indicated. **D**, Pull-down assay of [³⁵S]-labeled chimeric growth factors electrophoresed in SDS-PAGE in reducing and nonreducing conditions. **E**, Determination of dual-binding specificity of VA1 protein. **F**, Covalent cross-linking of VEGFR-2 and Tie2 on blood vascular endothelial cells (BECs) in the presence of VA1 but not VEGF or Ang1 proteins. Serum-starved BECs were stimulated with the proteins for 20 minutes, rinsed, treated with 3,3'-Dithiobis(sulfosuccinimidylpropionate) (DTSSP, Thermo Scientific) for another 30 minutes and lysed. **G**, Nonreducing gel electrophoresis of VA1 and VEGF proteins expressed in Sf21 insect cells using the baculovirus expression system and purified to homogeneity. The proteins were stained with Coomassie. **H**, Cell survival assay using methylthiazolyldiphenyl-tetrazolium bromide with Sf21-expressed and purified VA1 and VEGF proteins. Details of the assay are described in Methods in the online-only Data Supplement.

umbilical vein endothelial cells that contain Tie2, washed again, and subjected to gel electrophoresis and Western blotting with Tie2-specific antibodies. The results indicated that VA1, unlike VEGF, Ang1, or control medium, is able to simultaneously bind to both receptors (Figure 1E).

The receptor-binding properties of VA1 were also characterized in cultured human umbilical vein endothelial cells expressing a Tie2–green fluorescent protein fusion protein.²³ Ang1 treatment of these cells led to an accumulation of Tie2–green fluorescent protein in cell-cell junctions (arrows in Figure 1B in the online-only Data Supplement and References 23 and 24). In similar conditions, VA1 (but not VEGF) produced in mammalian cells also led to Tie2 accumulation in cell-cell junctions, whereas the purified dimeric VA1 from insect cells gave less junctional Tie2–green fluorescent protein signal in this assay (Figure 1B in the online-only Data Supplement and data not shown).

Covalent cross-linking was used to further demonstrate the ability of VA1 to “bridge” VEGFR-2 and Tie2 in human primary endothelial cells. Blood vascular endothelial cells (BECs) were first serum starved and then treated with VA1, VEGF, or Ang1 for 20 minutes, followed by application of the cross-linking reagent for 30 minutes. The cells were lysed, and solubilized proteins were immunoprecipitated with anti-VEGFR-2 antibodies and Western blotted with anti-Tie2. VEGFR-2/Tie2 cross-linking was observed only in the presence of VA1 (Figure 1F).

We next studied whether the chimeric proteins could bind to and induce activation of VEGFRs in a cell-based assay. Mouse pro-B myelocytic leukemia cells BaF3, stably expressing human VEGFR-1/EpoR fusion receptor or VEGFR-2/EpoR fusion receptor, were stimulated with serial dilutions of purified VA1 and VEGF proteins. Both VA1 and VEGF stimulated cell proliferation/survival in this assay, although the activity varied depending on the cell line used (Figure 1G and H). Similar results were obtained with media from 293T cells expressing VA1 or VEGF (data not shown).

Receptor-Activating Properties of VA Chimeric Proteins

We next analyzed receptor-activating properties of the VA proteins in more detail. Similar to VEGF, both chimeric proteins activated VEGFR-2 phosphorylation in human umbilical vein endothelial cells and BECs (Figure 2A and 2B). Both chimeric proteins also stimulated Tie2 phosphorylation, although significantly less than Ang1, used as a positive control in this assay (Figure 2A). The reduced activity of the VA chimeras in the Tie2 phosphorylation assay resembled that of Ang2 (Figure 1VA in the online-only Data Supplement and elsewhere^{23,25}), perhaps because of similar dimeric structures of the VA and Ang2 proteins, differentiating them from the multimeric structures of Ang1 and COMP-Ang1.²⁰ Because both VA forms behaved similarly in the above assays, only the linker-containing isoform VA1 was used in subsequent studies.

The above experiments demonstrated that although VA1 is able to bind to and activate VEGFR-2, it can simultaneously bind to (and weakly activate) Tie2, thus bridging the 2 receptors together. To address the question of how VA1 signals compared with VEGF, we first analyzed VEGFR-2 phosphorylation in cultured endothelial cells under continuous stimulation with the ligands for various periods of time. In these conditions,

VA1 and VEGF were equally active in stimulating VEGFR-2 phosphorylation. Either treatment also resulted in transient phosphorylation of the mitogen-activated protein kinases Erk1 and Erk2 (Figure 1IA in the online-only Data Supplement).

Because continuous stimulation of the cells with high ligand concentrations did not reveal significant differences between VA1 and VEGF, we undertook an experimental setup in which BECs were stimulated with receptor-saturating amounts of VEGF or VA1 for 5 minutes, then extensively rinsed with temperature- and CO₂-equilibrated serum-free medium, and further incubated for various periods of time in serum-free medium without the growth factors. Tyrosine phosphorylation of VEGFR-2 and Erk1/2 was then analyzed from the cell lysates by Western blotting. In these conditions, VEGF stimulated VEGFR-2 phosphorylation at Tyr1175 for a significantly longer time period than VA1 (Figure 2B). The difference was even more evident when the cells were stimulated with the mammalian cell–derived ligands and total phosphotyrosines of VEGFR-2 were determined (Figure 1IB in the online-only Data Supplement). As another control, we used a combined VEGF+Ang1 stimulation of BECs to find out whether the mere Tie2 activation was responsible for the differential VEGFR-2 phosphorylation. However, the addition of Ang1 did not affect VEGF-induced VEGFR-2 phosphorylation (Figure 1IB in the online-only Data Supplement). Compared with VEGF, VA1 treatment also resulted in less downregulation of the total VEGFR-2 protein in endothelial cells (Figure 2B and Figure 1IB in the online-only Data Supplement). Despite these differences, the duration of Erk1/2 phosphorylation differed only minimally between the cells stimulated with the 2 ligands, resembling the Erk1/2 phosphorylation response after continuous stimulation (Figure 1IA and 1IB in the online-only Data Supplement).

To characterize downstream signaling events after endothelial cell stimulation with the ligands, we analyzed the phosphorylation of several secondary messengers such as p38, docking protein-2 (DokR), cAMP response element binding protein (CREB), and endothelial nitric oxide synthase. Compared with VEGF, VA1 induced a more transient increase in p38 and CREB phosphorylation, whereas DokR and endothelial nitric oxide synthase were equally phosphorylated after stimulation with both factors (Figure 1IC and 1ID in the online-only Data Supplement and data not shown).

The reduced ability of VA1 to stimulate VEGFR-2 degradation compared with VEGF prompted us to use 2 different approaches in which VEGFR-2 downregulation could be observed more directly. BECs were transduced with retroviruses encoding a VEGFR-2–cyan fluorescent protein fusion protein and stimulated with VA1, VEGF, or Ang1, and receptor internalization was analyzed 45 minutes later. The formation of VEGFR-2–cyan fluorescent protein containing intracellular vesicles was strongly induced by VEGF but very weakly induced by VA1 or Ang1 (Figure 1IE in the online-only Data Supplement).

In another approach, we used BECs stimulated with VA1, VEGF, Ang1, or VEGF+Ang1 for 10 minutes. The incubation was then continued in fresh medium without growth factors for 30 minutes; cell-surface proteins were biotinylated; the cells were lysed; and biotinylated proteins were bound to streptavidin-agarose and subjected to Western blotting for VEGFR-2. As expected, VEGF led to downregulation of the VEGFR-2

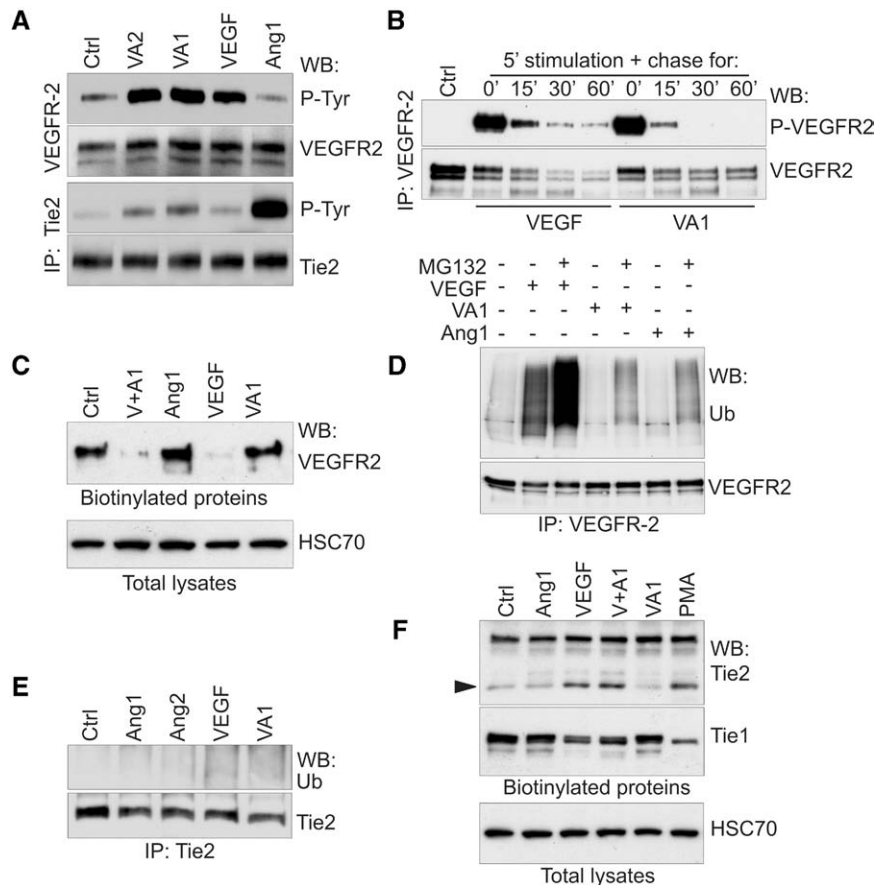


Figure 2. Receptor activation and downstream signaling by VA1. **A**, Human umbilical vein endothelial cells were stimulated with the indicated ligands produced in 293T cells for 10 minutes and lysed, and vascular endothelial growth factor (VEGF) receptor (VEGFR)-2 and Tie2 were analyzed by Western blotting for phosphotyrosine (P-Tyr), VEGFR-2, or Tie2.

B, Phosphorylation of VEGFR-2 (Tyr1175) after stimulation of blood vascular endothelial cells (BECs) with purified VEGF or VA1 proteins produced in Sf21 insect cells for 5 minutes, rinsing, and further incubation in medium without ligands for the indicated periods of time. WB indicates Western blot. **C**, VA1 promotes less internalization of VEGFR-2 than VEGF (V). Serum-starved BECs were stimulated with the indicated factors for 10 minutes, rinsed, and further incubated for 30 minutes. Surface proteins were biotinylated, and VEGFR-2 was analyzed as described in Method. **A** indicates angiotensin. **D** and **E**, VA1 induces less ubiquitinylation of VEGFR-2 than VEGF and no Tie2 ubiquitinylation. Serum-starved BECs were stimulated for 10 minutes; VEGFR-2 or Tie2 was immunoprecipitated; and ubiquitinated receptor proteins were visualized by Western blotting. **F**, VA1 does not induce internalization of Tie2 or Tie1. The experiment was performed essentially as described in **C**, but surface Tie2 and Tie1 were analyzed instead.

available for biotinylation on the cell surface because of receptor internalization, whereas VA1 or Ang1 treatment did not significantly alter cell-surface expression of VEGFR-2 (Figure 2C).

We also analyzed whether VEGFR-2 was covalently modified by polyubiquitinylation for degradation in the proteasome after these treatments. BECs were stimulated for 10 minutes, lysed, and VEGFR-2 immunoprecipitated. Western blotting with anti-ubiquitin antibodies indicated that VEGF but not VA1 or angiotensins induced polyubiquitinylation of VEGFR-2 (Figure 2D). The proteasome inhibitor MG132 was used in this experiment to prevent VEGFR-2 degradation to increase the sensitivity of the assay. In similar conditions, Tie2 was not ubiquitinated (Figure 2E).

It has been demonstrated that VEGF is able to induce Tie2 ectodomain shedding, thus modulating Tie2 signaling.²⁶ VEGF has also been shown to stimulate Tie1 ectodomain shedding.²⁷ To analyze whether VA1 stimulates the ectodomain cleavages, BECs were stimulated with VA1, VEGF, Ang1, or VEGF+Ang1 (or phorbol-12-myristate-13-acetate (PMA) as a strong positive control),²⁶ and biotinylated BEC cell-surface proteins were analyzed by Western blotting for Tie2 and Tie1. VEGF alone or in combination with Ang1 led to Tie2 cleavage, releasing a 75-kDa fragment recognized by the anti-Tie2 antibodies (arrowhead in Figure 2F). In contrast, VA1 or Ang1 did not affect Tie2 expression or cleavage. Ang2 treatment was similarly inactive in the ectodomain cleavage assay (data not shown). VEGF (but not VA1, Ang1, or Ang2) also led to a small decrease in the amount of the intact cell-surface Tie1 receptor (Figure 2F and data not shown).

We next analyzed whether VE-cadherin phosphorylation and internalization differ between cells treated with VA1 and VEGF because VE-cadherin constitutes one of the key mechanisms maintaining vascular integrity in blood vessels.²⁸ Human umbilical vein endothelial cells were treated with VA1, VEGF, Ang1, Ang2, or BSA, and VE-cadherin Tyr658 phosphorylation was determined. VEGF increased the phosphorylation slightly, whereas VA1 or the VEGF+Ang1 combination induced strong VE-cadherin phosphorylation ($P<0.05$; Figure 3A and Figure III in the online-only Data Supplement). Strikingly, unlike VEGF, VA1 or the VEGF+Ang1 combination restored the initial downregulation of cell-surface VE-cadherin at the 30-minute time point (Figure 3B). Consistent with this, Src phosphorylation, which is involved in VEGF/VEGFR2-stimulated VE-cadherin phosphorylation and internalization,²⁹ was strongly increased by VEGF but was increased very little by VA1 or VEGF+Ang1 (Figure 3C and Figure IIIB in the online-only Data Supplement).

VA1 Induces Angiogenesis With a Distinct Vessel Pattern in Skeletal Muscle and Skin

Because VA1 was able to stimulate VEGFR-2 and downstream kinases (such as extracellular signal-regulated kinase [Erk]-1/2) but showed differences in VEGFR-2 activation and downregulation kinetics, we wanted to analyze the angiogenic activity of VA1 versus VEGF in vivo. rAAVs encoding VA1, VEGF, Ang1, or the control protein (human serum albumin) were injected into tibialis anterior muscles of FVB/N mice at the dose of 8×10^9 vector genomes per muscle. The muscle

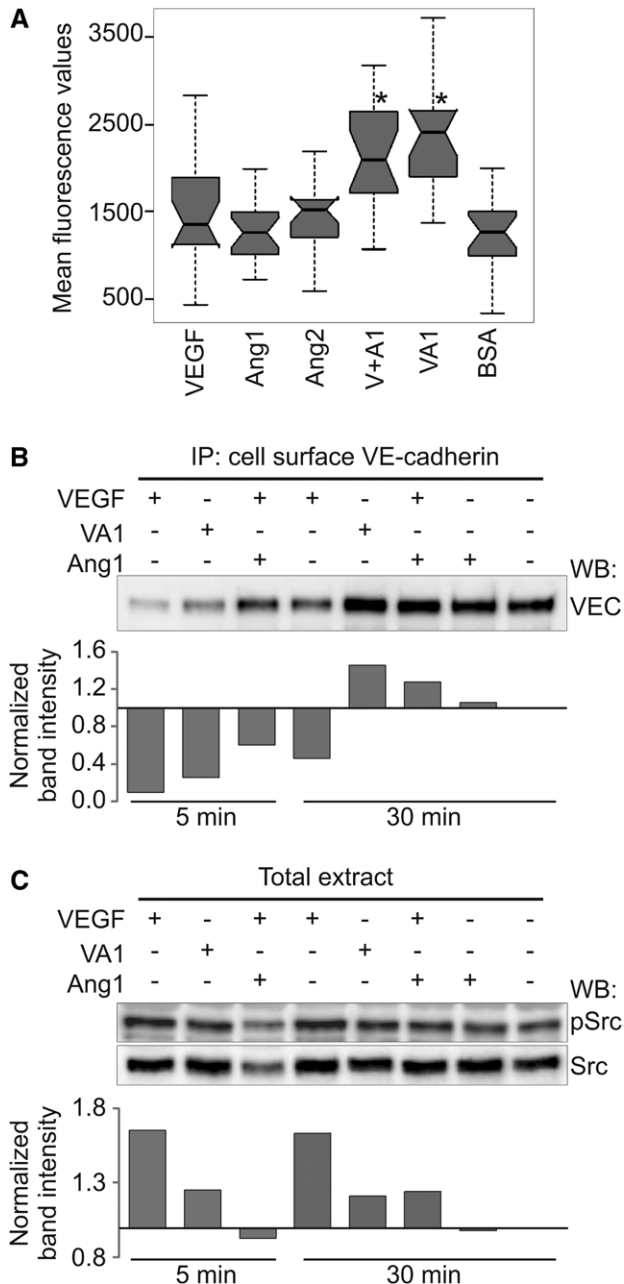


Figure 3. Effect of VA1 on cell surface VE-cadherin and Src phosphorylation. **A**, VA1 induces VE-cadherin Tyr658 phosphorylation. Human umbilical vein endothelial cells (HUVECs) were grown to confluence, serum starved, stimulated with the indicated proteins, fixed, permeabilized, and stained with affinity-purified rabbit antibody to phosphorylated (P) Tyr658 of VE-cadherin. The fluorescence was quantified and statistically analyzed as shown in the plot. Representative images are shown in Figure III in the online-only Data Supplement. **A** indicates angiopoietin; and V, vascular endothelial growth factor (VEGF). **B**, VA1 induces less internalization of VE-cadherin than VEGF. HUVECs, grown to confluence, were incubated with mouse monoclonal BV-6 antibody (mAb) directed against the VE-cadherin extracellular domain, rinsed, and treated with the indicated proteins for 5 or 30 minutes. Cell-surface VE-cadherin was then analyzed by Western blotting (WB) in cell lysates. **C**, VA1 induces less Src phosphorylation than VEGF. The conditions used were as described in **B**. In **A**, ANOVA followed by Dunnett post hoc test was used. Error bars indicate mean \pm SD. * P <0.05.

vasculature was analyzed at 1 to 4 weeks. Four days after the injections, transgene-encoded protein expression was confirmed by ELISA in the muscle. VEGF and VA1 concentrations were 0.79 ± 0.3 and 1.64 ± 0.2 ng/mg tissue, respectively, indicating similar molar concentrations. Quantification of VEGF and VA1 protein expression at the very late time point (5 weeks after injection) showed that the proteins were expressed continuously in the treated muscles at similar levels (data not shown).

Antibody staining of frozen muscle sections for the endothelial marker platelet endothelial cell adhesion molecule-1 (Figure 4A and 4B, 4 weeks; Figure VA in the online-only Data Supplement, quantification for 1–4 weeks) and Doppler ultrasound analysis of the rAAV-treated muscles (Figure 4C and 4D) demonstrated that VA1 retained the angiogenic (P <0.01) and perfusion-increasing (P <0.05) activities of VEGF. However, fluorescent (DiI) staining of the vessels via cardiac perfusion revealed distinct vascular patterns in the muscles treated with VA1 versus VEGF (Figure 4E). Whereas VEGF induced an angioma-like pattern consisting of enlarged vessels concentrated in “glomeruloid tufts” (see also the work by Carmeliet³⁰), the VA1-induced vessels were more dilated and evenly distributed. Human serum albumin, used as a control, did not have any angiogenic effect in these conditions. Ang1 and Ang2 induced a minor increase in the platelet endothelial cell adhesion molecule-1–positive endothelial area, although Ang1 treatment did not increase perfusion (Figure 4A–D and Figure IVB and IVC in the online-only Data Supplement).

To characterize further the maturation of the vessels induced by these treatments, we stained muscle sections for markers expressed by pericytes and smooth muscle cells (chondroitin sulfate proteoglycan NG2, platelet-derived growth factor receptor- β , and α -smooth muscle actin, respectively). Quantification of the stained areas indicated that pericyte/smooth muscle cell coverage of the induced vessels was comparable between the VA1 and VEGF groups (Figure 4A and B and Figures VA, VIA, and VIB in the online-only Data Supplement). Interestingly, the blood capillaries induced by VA1 appeared more regular than those induced by VEGF. This finding corresponds to the vessel pattern observed by DiI staining (compare the VA1 and VEGF panels in Figure 4E and Figure VIA in the online-only Data Supplement).

Immunohistochemical analysis of blood vessels in mouse skin after the injection of recombinant rAAVs demonstrated increased sprout formation and branching in VA1-treated samples compared with the VEGF-treated samples. Furthermore, rAAV-VEGF-induced angioma-like formations were not observed with rAAV-VA1 (Figure VII in the online-only Data Supplement).

VA1 Induces Less Permeability in Skeletal Muscle

To characterize vessel permeability in the transfected muscles, the Miles assay was used. In this assay, VEGF induced significant extravasation of the Evans Blue dye from the vessels of FVB/N mice after 1, 2, or 3 weeks, whereas the vascular permeability in the VA1-transfected muscle was significantly (P <0.001) lower (Figure 5A and B, Figure VD in the online-only Data Supplement, and data not shown). Doubling of the virus dose did not result in increased Evans Blue extravasation at 1 or 2 weeks; only a minor increase occurred at 3

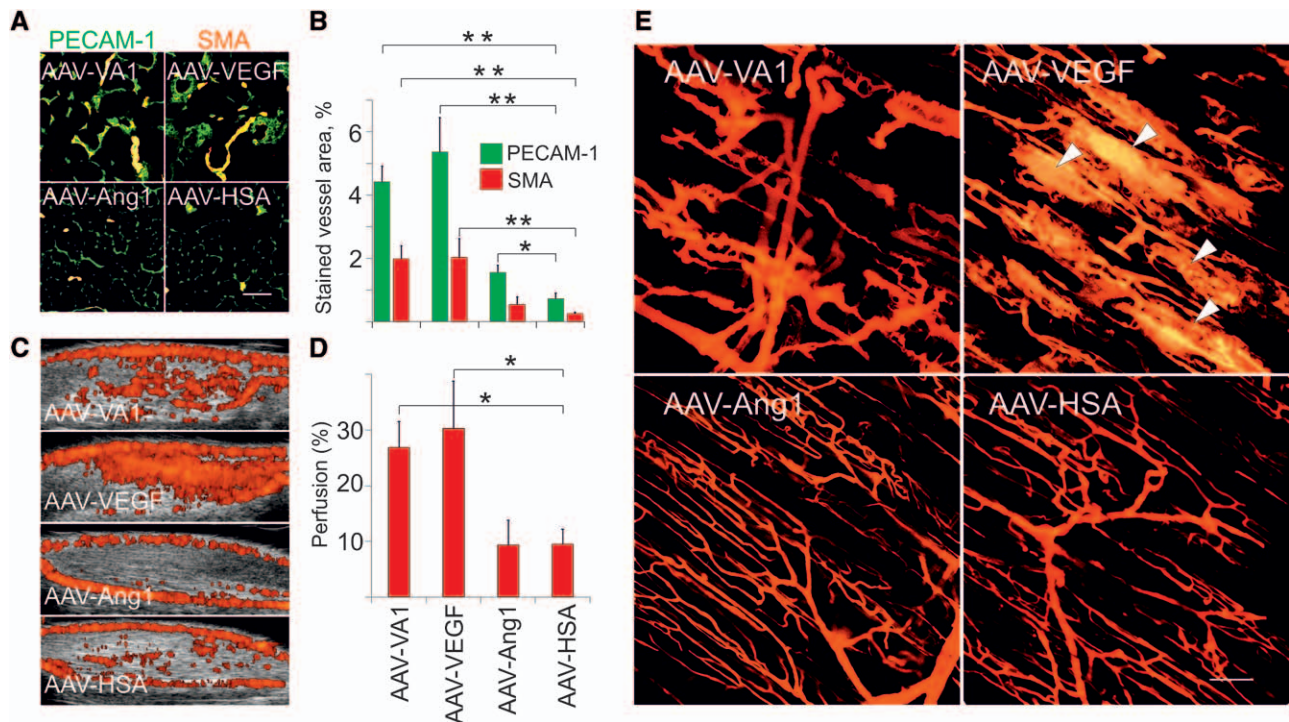


Figure 4. Vascular effects of VA1 in skeletal muscle. VA1, vascular endothelial growth factor (VEGF), angiopoietin (Ang)-1, and human serum albumin (HSA) were expressed in mouse skeletal muscle via recombinant adeno-associated viral (rAAV) delivery. **A**, Representative immunohistochemical images of platelet endothelial cell adhesion molecule-1 (PECAM-1) and smooth muscle actin (SMA)-stained tibialis anterior muscle sections from FVB/N female mice transduced with the indicated rAAVs for 3 weeks. **B**, Quantification data from the immunohistochemical staining. **C**, Representative images of blood vessel perfusion analyzed by Doppler ultrasound. **D**, Quantification data from the ultrasound (based on 3-dimensional projections). Data are representative of 4 (**A**) and 2 (**C**) independent experiments. In **B** and **D**, ANOVA followed by Dunnett post hoc test was used. Error bars indicate mean \pm SD. * $P\leq 0.05$; ** $P\leq 0.01$. Bar in **A**=100 μ m. **E**, Direct visualization of tibialis anterior blood vessels treated with the indicated rAAVs for 2 weeks, using cardiac perfusion with Dil as described in Methods. **White arrowheads** indicate angioma-like vascular patterns.

weeks (Figure 5B). Ang1 expression led to decreased dye extravasation, as previously published,¹⁵ and Ang2 had no effect (Figures IVD and VD in the online-only Data Supplement). Compared with VEGF, VA1 also induced less Evans Blue extravasation in an acute vessel permeability test in the skin (data not shown). Further analysis of the treated muscles demonstrated that VA1 induced significantly less leukocyte recruitment to the muscles than VEGF (Figure VB and VC in the online-only Data Supplement and data not shown).

VA1 Improves Perfusion in a Mouse Hind-limb Ischemia Model

To test the ability of VA1 to promote vessel growth in ischemic tissue, we used the mouse hind-limb ischemia model, involving a ligation closure of the femoral artery.³¹ When immunodeficient mice are used in this model, limb survival requires an angiogenic inducer, whereas in immunocompetent Balb/c mice, the operated limbs often survive without such treatment, perhaps because of better spontaneous collateral growth. Therefore, we selected immunodeficient mice for the experiment to get a clearer readout of the results. We found that rAAV-VEGF transduction of the muscle was not effective in protecting the limb from necrosis (perhaps because of induction of angioma formation), whereas rAAV-VA1 improved blood flow restoration and protected the operated limb from necrosis ($P<0.001$; Figure 5C and D).

Continuous expression of a transgenic protein such as VEGF in the rAAV-transduced tissue can cause abnormally

high local concentrations, resulting in tissue damage rather than healing. To avoid this limitation and to perform the experiment in a more clinically relevant fashion, hind-limb ischemia was induced in immunocompetent Balb/c mice as indicated above, but purified proteins instead of the rAAVs were delivered. Single injections of equimolar amounts of the indicated proteins were done after the surgery, and blood perfusion was measured after 3 and 7 days, as described in the expanded Methods and Materials section in the online-only Data Supplement. The results showed that even such short pulses of either VA1 or VEGF improve blood perfusion in the operated limbs ($P<0.05$), with a small trend for VA1 to provide better perfusion (Figure 6A and B).

VA1 and VEGF Show Distinct Signaling Properties In Vivo

Results from the hind-limb ischemia model using a single injection of the proteins suggested that the treatment would provide a relatively long-lasting signal to initiate capillary growth. To analyze the signaling properties of VA1 and VEGF proteins in mouse tissues, we injected equimolar amounts of the proteins to the blood circulation of FVB/N mice and analyzed their concentration kinetics in serum and in the lung and phosphorylation of VEGFR-2 (Y1175) and the downstream Akt (S473) kinase in the lung. Lung was chosen for analysis because it is a highly vascularized tissue that provides clear signals. The injected ligands were cleared rapidly from the blood circulation. However, VA1 was retained in the lungs at a higher level

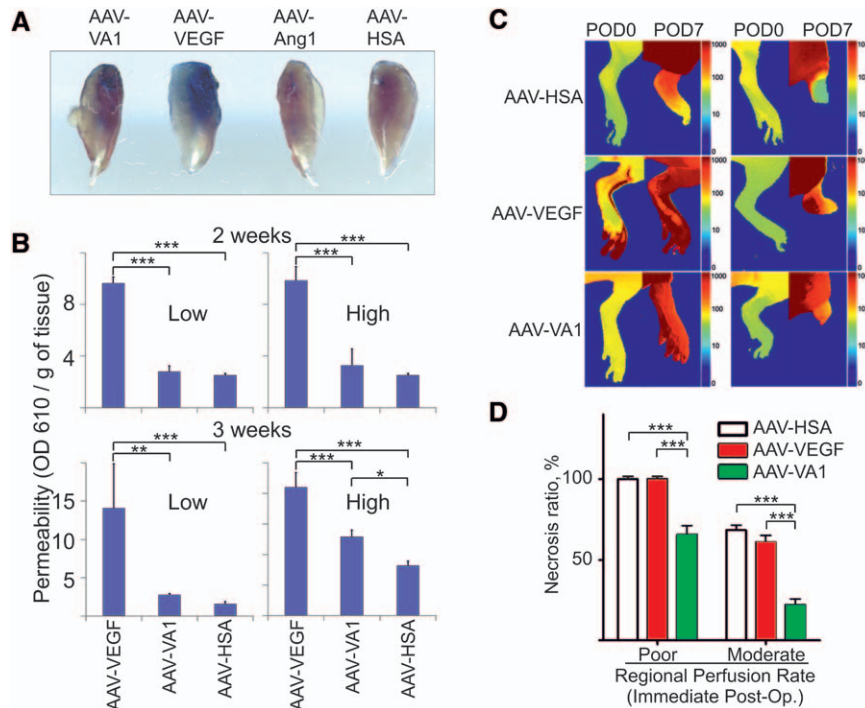


Figure 5. VA1 induces less vascular permeability but more vascular perfusion in ischemic hind limb than vascular endothelial growth factor (VEGF) when delivered via recombinant adeno-associated viral (rAAV). **A**, Representative images of Evans Blue staining in tibialis anterior muscles treated with the indicated rAAVs for 2 weeks. Ang1 indicates angiotensin-1; and HSA, human serum albumin. **B**, Quantification of data from the Miles permeability assay 2 and 3 weeks after rAAV transduction. Two virus doses were tested (low, -8×10^9 viral particles; high, -1.34×10^{10} viral particles) in 30 μ L per muscle. ANOVA followed by the Tukey post hoc test was used. **C**, Tissue perfusion and ratio of necrosis in ischemic hind limbs treated with the indicated rAAVs. The regional tissue perfusion rate (%/min) was defined as the fraction of blood exchanged per minute in the vascular volume by time-series analysis of indocyanine green dye. Blood perfusion rate in the hind limb was measured at postoperative days (PODs) 0 and 7. The representative perfusion rate map and pseudo-scale bar are indicated in log scale. **D**, Correlation between regional perfusion rates of the ischemic hind limbs at POD 0 and limb necrosis levels at POD 7. The x axis shows the regional perfusion rate of the ischemic hind limbs (poor perfusion rate, 0%/min–30%/min; moderate perfusion rate, 30%/min–80%/min). Normal hind limbs typically demonstrate a perfusion rate >500 %/min. Shown are the best and the worst cases in each experimental group. ANOVA followed by Dunnett post hoc test was used. Error bars indicate SD. * $P < 0.05$; ** $P < 0.01$; *** $P < 0.001$.

and for a significantly longer time than VEGF (Figure 6C). Analysis of the lung lysates indicated that VEGFR-2 was tyrosine phosphorylated in both experimental groups. Compared with VEGF, VA1 led to slower VEGFR-2 downregulation (Figure 6D). Furthermore, VA1 (or the VEGF+Ang1 combination) stimulated phosphorylation of Akt more strongly than VEGF in the lung and in cultured BECs (Figure 6E).

Discussion

In this work, we describe the chimeric VEGF-Ang1 growth factor VA1, designed by combining the receptor-binding domains of VEGF and Ang1. We show that VA1 retains the angiogenic properties of VEGF but induces significantly fewer angioma-like structures, less vessel permeability, and less inflammation in mouse skeletal muscle. In ischemic skeletal muscle, VA1, delivered via rAAVs, showed clear benefits over VEGF in restoring blood flow and rescuing the limb from necrosis.

The angiogenic activity of VEGF is known to be mediated mainly via the activation of VEGFR-2.⁶ In fact, ligands activating only VEGFR-2 such as VEGF-E and one of the VEGF-D isoforms are able to induce an angiogenic response.^{6,12} In endothelial cell cultures, both VEGF and VA1 stimulated strong VEGFR-2 phosphorylation, but differences were found in the phosphorylation kinetics of VEGFR-2, the serine/threonine-specific protein kinase Akt, the Src tyrosine kinase, the

mitogen-activated protein kinases Erk1/2, p38, and the CREB transcription factor after VEGF versus VA1 stimulation. After short-term stimulation followed by removal of the unbound ligand and further incubation, VEGF induced a more prolonged phosphorylation of VEGFR-2 than VA1. Compared with VA1, VEGF also induced more VEGFR-2 ubiquitinylation and faster VEGFR-2 degradation.

To gain mechanistic insight into the differential properties of VEGF and VA1, we used several biochemical and cellular assays. Binding studies confirmed that VA1 binds VEGFR-2, Tie-2, and VEGFR-1. The affinity of VA1 for VEGFR-2 was comparable to that of VEGF²² and, for Tie2, similar to the Ang-1 fibrinogen-like domain.³² Furthermore, unlike VEGF, VA1 could simultaneously bind to both VEGFR-2 and Tie2, being capable of establishing a molecular link between these 2 major endothelial growth factor receptors *in trans* or *in cis*. This result was confirmed in cross-linking experiments using cultured endothelial cells. Compared with VEGFR-2, Tie2 is known to be internalized slowly and to be involved in multimeric *in trans* complexes stabilizing endothelial cell-cell contacts.^{23,24} Thus, the bivalent ligand VA1, via binding to both VEGFR-2 and Tie2, could establish multimeric complexes in which VEGFR-2 internalization and subsequently ubiquitinylation are significantly delayed. This conclusion was substantiated by our cellular assays indicating that VA1

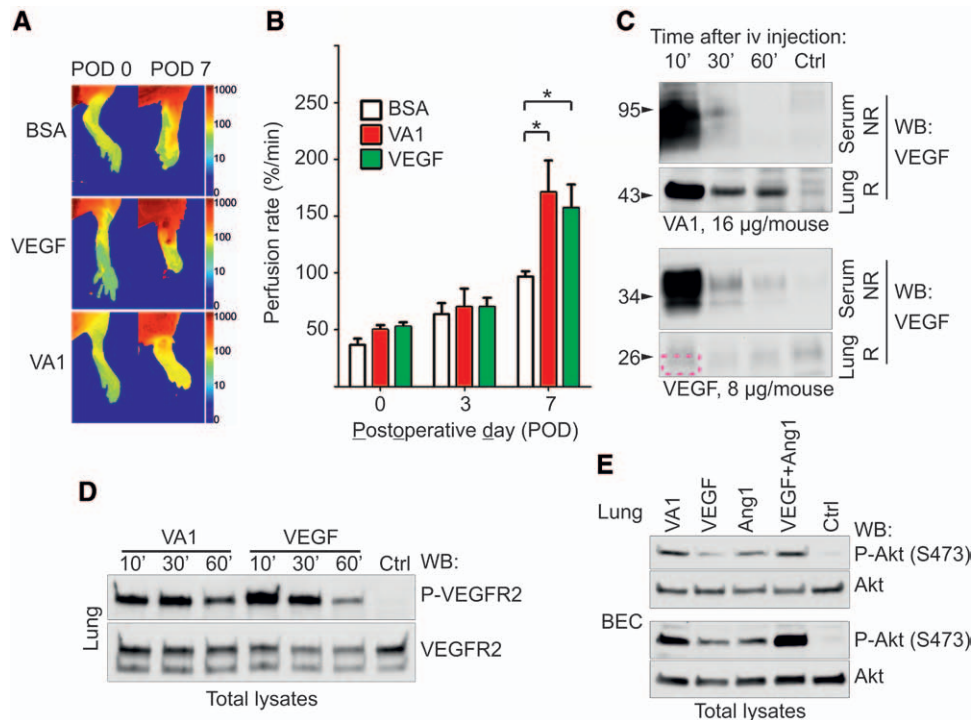


Figure 6. VA1 protein strongly induces blood perfusion in ischemic hind limb. **A**, After induction of hind-limb ischemia, the mice received a single intramuscular injection of the indicated proteins. Blood perfusion in the hind limbs was measured on postoperative days (PODs) 0, 3, and 7. **B**, Quantification of the data in **A**. **C**, Serum and lung concentration kinetics of VA1 and vascular endothelial growth factor (VEGF) injected into the tail vein at the indicated (equimolar) amounts. At the indicated time points after the injection, the mice were euthanized, and 5- μ L serum samples or 200 μ g of lung lysates was analyzed in nonreducing (NR) or reducing (R) conditions, respectively, by Western blotting (WB) using anti-VEGF antibodies. Red dotted square indicates the position of the VEGF band. **D**, Phosphorylation of VEGFR-2 (Y1175) and total VEGFR-2 proteins at various time points after VA1 or VEGF injection via the tail vein. **E**, Akt Ser473 phosphorylation in lungs 10 minutes after tail vein injection of the indicated ligands and in cultured blood vascular endothelial cells (BECs) stimulated for the same time period. In **B**, ANOVA followed by Dunnett post hoc test was used. * $P < 0.05$.

promoted very little accumulation of VEGFR-2-containing intracellular vesicles. In contrast, in the same assays, VEGF potently stimulated VEGFR-2 internalization and directed the receptor to proteasomal degradation. Unlike VEGF, VA1 did not induce Tie2 (or Tie1) cleavage in cultured endothelial cells, thus stabilizing heterotrimeric ligand-receptor complexes on the cell surface. This was also reflected in the long half-life of VA1 in the lung vasculature.

Short-time stimulation experiments indicated that VA1 versus VEGF treatment of endothelial cells results in distinct VEGFR-2 phosphorylation and internalization kinetics. The slow internalization and quick dephosphorylation of VEGFR-2 after short-time stimulation with VA1 suggest that it is dephosphorylated and inactivated by junctional phosphatases such as density-enhanced phosphatase-1.³³ Vascular endothelial protein tyrosine phosphatase, which becomes associated with Tie2 and VE-cadherin,³⁴ could also be involved in VEGFR-2 dephosphorylation. It is known that internalized VEGFR-2 remains in the endosomal compartments (sorting endosomes)³⁵ for some time, retaining its full activity.^{36,37} This was reflected in our assays on the biochemistry and internalization of VEGFR-2–cyan fluorescent protein. VEGFR-2–induced phosphorylation and disassembly of VE-cadherin of the adherens junctions is considered to be one of the key mechanisms of the VEGF-induced permeability response.^{36,38} VEGFR-2 can associate with VE-cadherin and, on VEGF stimulation,

induce its phosphorylation,³⁹ in part via an Src-Vav2-PAK-dependent mechanism.²⁸ In our experiments, we observed that VA1 induced VE-cadherin phosphorylation; however, this was not accompanied by its internalization, unlike with VEGF.

Stimulation of Tie2 by Ang1 was shown to counteract VEGF/VEGFR-2-mediated signaling and to maintain vascular integrity.^{15,40} Importantly, Ang1 can reduce plasma leakage and strengthen adult vasculature integrity even in the absence of mural cells.⁴¹ Ang1 can inhibit VEGF-induced activation of Src, thus inhibiting VE-cadherin internalization and rescuing the endothelial barrier function.²⁹ Consistent with the above results, less Src phosphorylation was detected after VA1 treatment than after VEGF treatment. Although VA1 is a less potent stimulator of Tie2 phosphorylation than Ang1, Tie2 phosphorylation by VA1 could contribute to the improved permeability properties of VA1 compared with VEGF. Furthermore, VEGF sustained CREB phosphorylation for a significantly longer time than VA1. Because this phosphorylation correlates with reduced VE-cadherin cell-surface expression and increased endothelial monolayer permeability response,⁴² it is also possible that VEGF downregulates VE-cadherin expression more than VA1.

Unlike VEGF, VA1 did not induce Tie2 or Tie1 ectodomain cleavage, thus providing an additional mechanism for the stabilization of heterotrimeric molecular complexes on endothelial cells. Furthermore, because leukocyte extravasation

can occur through endothelial gaps⁴³ and Ang1 can decrease plasma leakage by reducing the number and size of endothelial gaps,⁴⁴ the reduced vessel leakiness associated with VA1 could also result in decreased accumulation of inflammatory cells in the treated muscles.

We used 2 different hind-limb ischemia models employing femoral artery ligation to compare the therapeutic abilities of VA1 and VEGF to restore blood flow and to rescue the ischemic hind limb. The results showed a clear benefit of VA1 over VEGF when the therapeutic agents were delivered into the ischemic limb via rAAV. In the second model, using single injection of purified therapeutic proteins after the surgery, VA1 and VEGF were comparable in restoring blood perfusion, although VA1 showed a trend toward better performance. We could furthermore show that VA1 is retained in highly vascularized tissues better than VEGF and that it stimulates the antiapoptotic protein kinase Akt more efficiently than VEGF both in vitro and in vivo.

Reports published over the past decade have shown that the effect of VEGF in ischemic limb depends on its dose in the transduced muscle tissue, on the mouse strain, and on the delivery method.^{45–48} It was shown that lower or transient VEGF expression results in the formation of unstable vessels poorly covered by pericytes that are prone to regression.⁴⁹ On the contrary, higher and sustained VEGF expression can lead to angioma growth and poor perfusion, thus posing the challenge of finding an appropriate VEGF dose.^{47,50} The failure to obtain optimal VEGF expression could be a possible reason for the lack of a therapeutic effect when VEGF was delivered via rAAVs in the present study. On the other hand, an excess of VA1 may not be equally harmful because it induces less vascular leakage and inflammation, thus providing more flexibility for its practical use.

Conclusions

We have designed and characterized a chimeric molecule, VA1, that is strongly angiogenic in skeletal muscle but does not induce angioma-like growth, vascular permeability, or inflammatory cell recruitment to the same degree as VEGF. VA1 was found to be very effective in restoring blood flow and rescuing ischemic muscle in the mouse hind-limb model. These properties make VA1 an attractive alternative for proangiogenic gene therapy.

Acknowledgments

We thank Dr Miina Öhman and Maija Bry for comments on the manuscript, Tapio Tainola and Tanja Laakkonen for expert technical assistance, the rAAV Gene Transfer and Cell Therapy Core Facility of Biocentrum Finland for virus production, the Biomedicum Imaging Unit for microscope support, and the staff at the Biomedicum Helsinki and the Haartman Institute Animal Facilities for excellent animal husbandry.

Sources of Funding

This study was supported by the Academy of Finland Collaborative Research Consortium on Genome-Scale Cancer Biology (decision number 262976) and the Council of Health (130446 to Dr Saharinen), European Research Council (TX-FACTORS, grant ERC-2010-AdG-268804), the Leducq Transatlantic Network of Excellence (Lymph Vessels in Obesity and Cardiovascular Disease), the Sigrid Juselius Foundation, and Biocenter Finland. Dr E. Dejana and F. Orsenigo were supported by Associazione Italiana per la Ricerca sul Cancro and “Special Program Molecular Clinical Oncology 5x1000” to the AIRC-Gruppo Italiano Malattie Mieloproliferative.

Disclosures

None.

References

- Ferrara N. Vascular endothelial growth factor. *Arterioscler Thromb Vasc Biol.* 2009;29:789–791.
- Carmeliet P. Angiogenesis in life, disease and medicine. *Nature.* 2005;438:932–936.
- Adams RH, Alitalo K. Molecular regulation of angiogenesis and lymphangiogenesis. *Nat Rev Mol Cell Biol.* 2007;8:464–478.
- Gupta R, Tongers J, Losordo DW. Human studies of angiogenic gene therapy. *Circ Res.* 2009;105:724–736.
- Nagy JA, Benjamin L, Zeng H, Dvorak AM, Dvorak HF. Vascular permeability, vascular hyperpermeability and angiogenesis. *Angiogenesis.* 2008;11:109–119.
- Shibuya M, Claesson-Welsh L. Signal transduction by VEGF receptors in regulation of angiogenesis and lymphangiogenesis. *Exp Cell Res.* 2006;312:549–560.
- Inoue N, Kondo T, Kobayashi K, Aoki M, Numaguchi Y, Shibuya M, Murohara T. Therapeutic angiogenesis using novel vascular endothelial growth factor-E/human placental growth factor chimera genes. *Arterioscler Thromb Vasc Biol.* 2007;27:99–105.
- Bry M, Kivellä R, Holopainen T, Anisimov A, Tammela T, Soronen J, Silvola J, Saraste A, Jeltsch M, Korpisalo P, Carmeliet P, Lemström KB, Shibuya M, Ylä-Herttuala S, Alhonen L, Mervaala E, Andersson LC, Knutu J, Alitalo K. Vascular endothelial growth factor-B acts as a coronary growth factor in transgenic rats without inducing angiogenesis, vascular leak, or inflammation. *Circulation.* 2010;122:1725–1733.
- Rissanen TT, Markkanen JE, Gruchala M, Heikura T, Puranen A, Ketunen MI, Kholová I, Kauppinen RA, Achen MG, Stacker SA, Alitalo K, Ylä-Herttuala S. VEGF-D is the strongest angiogenic and lymphangiogenic effector among VEGFs delivered into skeletal muscle via adenoviruses. *Circ Res.* 2003;92:1098–1106.
- Anisimov A, Alitalo A, Korpisalo P, Soronen J, Kaijalainen S, Leppänen VM, Jeltsch M, Ylä-Herttuala S, Alitalo K. Activated forms of VEGF-C and VEGF-D provide improved vascular function in skeletal muscle. *Circ Res.* 2009;104:1302–1312.
- Keskitalo S, Tammela T, Lyytikka J, Karpanen T, Jeltsch M, Markkanen J, Ylä-Herttuala S, Alitalo K. Enhanced capillary formation stimulated by a chimeric vascular endothelial growth factor/vascular endothelial growth factor-C silk domain fusion protein. *Circ Res.* 2007;100:1460–1467.
- Leppänen VM, Jeltsch M, Anisimov A, Tvorogov D, Aho K, Kalkkinen N, Toivanen P, Ylä-Herttuala S, Ballmer-Hofer K, Alitalo K. Structural determinants of vascular endothelial growth factor-D receptor binding and specificity. *Blood.* 2011;117:1507–1515.
- Augustin HG, Koh GY, Thurston G, Alitalo K. Control of vascular morphogenesis and homeostasis through the angiopoietin-Tie system. *Nat Rev Mol Cell Biol.* 2009;10:165–177.
- Kim I, Moon SO, Park SK, Chae SW, Koh GY. Angiopoietin-1 reduces VEGF-stimulated leukocyte adhesion to endothelial cells by reducing ICAM-1, VCAM-1, and E-selectin expression. *Circ Res.* 2001;89:477–479.
- Thurston G, Suri C, Smith K, McClain J, Sato TN, Yancopoulos GD, McDonald DM. Leakage-resistant blood vessels in mice transgenically overexpressing angiopoietin-1. *Science.* 1999;286:2511–2514.
- Su H, Takagawa J, Huang Y, Arakawa-Hoyt J, Pons J, Grossman W, Kan YW. Additive effect of AAV-mediated angiopoietin-1 and VEGF expression on the therapy of infarcted heart. *Int J Cardiol.* 2009;133:191–197.
- Chen F, Tan Z, Dong CY, Chen X, Guo SF. Adeno-associated virus vectors simultaneously encoding VEGF and angiopoietin-1 enhances neovascularization in ischemic rabbit hind-limbs. *Acta Pharmacol Sin.* 2007;28:493–502.
- Kim KT, Choi HH, Steinmetz MO, Maco B, Kammerer RA, Ahn SY, Kim HZ, Lee GM, Koh GY. Oligomerization and multimerization are critical for angiopoietin-1 to bind and phosphorylate Tie2. *J Biol Chem.* 2005;280:20126–20131.
- Muller YA, Li B, Christinger HW, Wells JA, Cunningham BC, de Vos AM. Vascular endothelial growth factor: crystal structure and functional mapping of the kinase domain receptor binding site. *Proc Natl Acad Sci USA.* 1997;94:7192–7197.
- Cho CH, Kammerer RA, Lee HJ, Steinmetz MO, Ryu YS, Lee SH, Yasunaga K, Kim KT, Kim I, Choi HH, Kim W, Kim SH, Park SK, Lee GM, Koh GY. COMP-Ang1: a designed angiopoietin-1 variant with nonleaky angiogenic activity. *Proc Natl Acad Sci USA.* 2004;101:5547–5552.
- Xu Y, Yu Q. Angiopoietin-2, unlike angiopoietin-1, is incorporated into the extracellular matrix via its linker peptide region. *J Biol Chem.* 2001;276:34990–34998.

22. Leppänen VM, Prota AE, Jeltsch M, Anisimov A, Kalkkinen N, Strandin T, Lankinen H, Goldman A, Ballmer-Hofer K, Alitalo K. Structural determinants of growth factor binding and specificity by VEGF receptor 2. *Proc Natl Acad Sci USA*. 2010;107:2425–2430.
23. Saharinen P, Eklund L, Miettinen J, Wirkkala R, Anisimov A, Winderlich M, Nottebaum A, Vestweber D, Deutsch U, Koh GY, Olsen BR, Alitalo K. Angiopoietins assemble distinct Tie2 signalling complexes in endothelial cell-cell and cell-matrix contacts. *Nat Cell Biol*. 2008;10:527–537.
24. Fukuhara S, Sako K, Minami T, Noda K, Kim HZ, Kodama T, Shibuya M, Takakura N, Koh GY, Mochizuki N. Differential function of Tie2 at cell-cell contacts and cell-substratum contacts regulated by angiopoietin-1. *Nat Cell Biol*. 2008;10:513–526.
25. Yuan HT, Khankin EV, Karumanchi SA, Parikh SM. Angiopoietin 2 is a partial agonist/antagonist of Tie2 signaling in the endothelium. *Mol Cell Biol*. 2009;29:2011–2022.
26. Findley CM, Cudmore MJ, Ahmed A, Kontos CD. VEGF induces Tie2 shedding via a phosphoinositide 3-kinase/Akt dependent pathway to modulate Tie2 signaling. *Arterioscler Thromb Vasc Biol*. 2007;27:2619–2626.
27. Yabkowitz R, Meyer S, Black T, Elliott G, Merewether LA, Yamane HK. Inflammatory cytokines and vascular endothelial growth factor stimulate the release of soluble tie receptor from human endothelial cells via metalloprotease activation. *Blood*. 1999;93:1969–1979.
28. Gavard J, Gutkind JS. VEGF controls endothelial-cell permeability by promoting the beta-arrestin-dependent endocytosis of VE-cadherin. *Nat Cell Biol*. 2006;8:1223–1234.
29. Gavard J, Patel V, Gutkind JS. Angiopoietin-1 prevents VEGF-induced endothelial permeability by sequestering Src through mDia. *Dev Cell*. 2008;14:25–36.
30. Carmeliet P. VEGF gene therapy: stimulating angiogenesis or angiogenesis? *Nat Med*. 2000;6:1102–1103.
31. Kang Y, Choi M, Lee J, Koh GY, Kwon K, Choi C. Quantitative analysis of peripheral tissue perfusion using spatiotemporal molecular dynamics. *PLoS One*. 2009;4:e4275.
32. Davis S, Papadopoulos N, Aldrich TH, Maisonpierre PC, Huang T, Kovac L, Xu A, Leidich R, Radziejewska E, Rafique A, Goldberg J, Jain V, Bailey K, Karow M, Fandl J, Samuelsson SJ, Ioffe E, Rudge JS, Daly TJ, Radziejewski C, Yancopoulos GD. Angiopoietins have distinct modular domains essential for receptor binding, dimerization and superclustering. *Nat Struct Biol*. 2003;10:38–44.
33. Lampugnani MG, Zanetti A, Corada M, Takahashi T, Balconi G, Breviario F, Orsenigo F, Cattelino A, Kemler R, Daniel TO, Dejana E. Contact inhibition of VEGF-induced proliferation requires vascular endothelial cadherin, beta-catenin, and the phosphatase DEP-1/CD148. *J Cell Biol*. 2003;161:793–804.
34. Winderlich M, Keller L, Cagna G, Broermann A, Kamenyeva O, Kiefer F, Deutsch U, Nottebaum AF, Vestweber D. VE-PTP controls blood vessel development by balancing Tie-2 activity. *J Cell Biol*. 2009;185:657–671.
35. Gampel A, Moss L, Jones MC, Brunton V, Norman JC, Mellor H. VEGF regulates the mobilization of VEGFR2/KDR from an intracellular endothelial storage compartment. *Blood*. 2006;108:2624–2631.
36. Lampugnani MG, Orsenigo F, Gagliani MC, Tacchetti C, Dejana E. Vascular endothelial cadherin controls VEGFR-2 internalization and signaling from intracellular compartments. *J Cell Biol*. 2006;174:593–604.
37. Lanahan AA, Hermans K, Claes F, Kerley-Hamilton JS, Zhuang ZW, Giordano FJ, Carmeliet P, Simons M. VEGF receptor 2 endocytic trafficking regulates arterial morphogenesis. *Dev Cell*. 2010;18:713–724.
38. Dejana E, Orsenigo F, Molendini C, Baluc P, McDonald DM. Organization and signaling of endothelial cell-to-cell junctions in various regions of the blood and lymphatic vascular trees. *Cell Tissue Res*. 2009;335:17–25.
39. Zanetti A, Lampugnani MG, Balconi G, Breviario F, Corada M, Lanfranccone L, Dejana E. Vascular endothelial growth factor induces SHC association with vascular endothelial cadherin: a potential feedback mechanism to control vascular endothelial growth factor receptor-2 signaling. *Arterioscler Thromb Vasc Biol*. 2002;22:617–622.
40. Nambu H, Nambu R, Oshima Y, Hackett SF, Okoye G, Wiegand S, Yancopoulos G, Zack DJ, Campochiaro PA. Angiopoietin 1 inhibits ocular neovascularization and breakdown of the blood-retinal barrier. *Gene Ther*. 2004;11:865–873.
41. Uemura A, Ogawa M, Hirashima M, Fujiwara T, Koyama S, Takagi H, Honda Y, Wiegand SJ, Yancopoulos GD, Nishikawa S. Recombinant angiopoietin-1 restores higher-order architecture of growing blood vessels in mice in the absence of mural cells. *J Clin Invest*. 2002;110:1619–1628.
42. Devi TS, Singh LP, Hosoya K, Terasaki T. GSK-3 β /CREB axis mediates IGF-1-induced ECM/adhesion molecule expression, cell cycle progression and monolayer permeability in retinal capillary endothelial cells: implications for diabetic retinopathy. *Biochim Biophys Acta*. 2011;1812:1080–1088.
43. van Wetering S, van den Berk N, van Buul JD, Mul FP, Lommerse I, Mous R, ten Klooster JP, Zwaginga JJ, Hordijk PL. VCAM-1-mediated Rac signaling controls endothelial cell-cell contacts and leukocyte transmigration. *Am J Physiol Cell Physiol*. 2003;285:C343–C352.
44. Baffert F, Le T, Thurston G, McDonald DM. Angiopoietin-1 decreases plasma leakage by reducing number and size of endothelial gaps in venules. *Am J Physiol Heart Circ Physiol*. 2006;290:H107–H118.
45. Fukino K, Sata M, Seko Y, Hirata Y, Nagai R. Genetic background influences therapeutic effectiveness of VEGF. *Biochem Biophys Res Commun*. 2003;310:143–147.
46. Urano T, Ito Y, Akao M, Sawa T, Miyata K, Tabata M, Morisada T, Hato T, Yano M, Kadomatsu T, Yasunaga K, Shibata R, Murohara T, Akaike T, Tanihara H, Suda T, Oike Y. Angiopoietin-related growth factor enhances blood flow via activation of the ERK1/2-eNOS-NO pathway in a mouse hindlimb ischemia model. *Arterioscler Thromb Vasc Biol*. 2008;28:827–834.
47. von Degenfeld G, Banfi A, Springer ML, Wagner RA, Jacobi J, Ozawa CR, Merchant MJ, Cooke JP, Blau HM. Microenvironmental VEGF distribution is critical for stable and functional vessel growth in ischemia. *FASEB J*. 2006;20:2657–2659.
48. Shimpo M, Ikeda U, Maeda Y, Takahashi M, Miyashita H, Mizukami H, Urabe M, Kume A, Takizawa T, Shibuya M, Ozawa K, Shimada K. AAV-mediated VEGF gene transfer into skeletal muscle stimulates angiogenesis and improves blood flow in a rat hindlimb ischemia model. *Cardiovasc Res*. 2002;53:993–1001.
49. Dor Y, Djonov V, Abramovitch R, Itin A, Fishman GI, Carmeliet P, Goelman G, Keshet E. Conditional switching of VEGF provides new insights into adult neovascularization and pro-angiogenic therapy. *EMBO J*. 2002;21:1939–1947.
50. Reginato S, Gianni-Barrera R, Banfi A. Taming of the wild vessel: promoting vessel stabilization for safe therapeutic angiogenesis. *Biochem Soc Trans*. 2011;39:1654–1658.

CLINICAL PERSPECTIVE

Insufficient vascular supply predisposes to tissue ischemia and infarction. Currently used treatments are based on surgical intervention and drugs that do not provide full recovery and may have side effects. New-generation therapies based on growth factor-stimulated angiogenesis provide exciting possibilities for improving the treatment of patients with tissue ischemia. However, the development of such therapies using, for example, the most potent angiogenic inducer, vascular endothelial growth factor (VEGF), is hindered by side effects such as angioma formation, vascular leakage, and inflammation, especially when used at high effective doses. On the other hand, low doses of VEGF stimulate the growth of unstable vessels, which are prone to regression after the therapy. Thus, the narrow range of effective concentrations of VEGF represents the main challenge for therapeutics development. Combined administration of growth factors such as VEGF and angiopoietin-1 to stimulate growth of more mature vessels has the disadvantages of unequal tissue distribution, different pharmacokinetic profiles, and higher cost compared with a single protein treatment. In the present study, we have developed a unique protein, called VA1, which combines the potent vessel growth stimulatory activity of VEGF and the permeability-inhibiting properties of angiopoietin-1. VA1 has a longer tissue half-life than VEGF; it strongly stimulates the antiapoptotic Akt pathway in endothelial cells; and it promotes vessel stability without angioma development. These properties make VA1 an attractive candidate for proangiogenic gene therapy.

SUPPLEMENTAL MATERIAL

Expanded Methods

Construction and production of the rAAV vectors.

The rAAV encoding VEGF₁₆₅ was published previously.¹ rAAVs encoding Ang1 and Ang2 were constructed in an analogous fashion. For the VA1 vectors, the fibrinogen-like domain (FLD) of human Ang1 was PCR-amplified using primers FLD-F (5'-TCGGTAGACCGAAGAAAGATAGAAGAGACTGTGCAGATGTATATC-3') and FLD-R (5'-CTCGGTAGACGAATTCTCAAAAATCTAAAGGTCGAATC-3'). To PCR-amplify FLD with a linker, FLD-linker-F primer (TCGGTAGACCGAAGAAAGATAGAATGGACACAGTCCACAACCT) and the above reverse primer were used instead. Both PCR products (containing 5' AccI site and 3' EcoRI and AccI sites) were digested with AccI and ligated into pKO-A165-AccI vector containing the VEGF homology domain (VHD) of VEGF, flanked by 5' EcoRI and 3' AccI sites. The resulting plasmid was opened with AccI and dephosphorylated. VA1 or VA2 inserts from the resulting plasmids were excised with EcoRI, blunted and ligated into the PmlI-opened psubCAG-WPRE rAAV vector (derivative of psubCMV-WPRE,² where the CMV promoter was replaced with the composite CAG promoter, consisting of the chicken beta-actin promoter, cytomegalovirus enhancer and beta-actin intron³). Production of rAAVs was carried out as previously described.¹

Protein expression and purification.

Angiopoietin-1, produced in mammalian cells or overexpressed in mice and COMP-Ang1 protein, purified from CHO cells,⁴ had similar biological activities and are collectively called here as Ang1. Purified VA1 protein with a C-terminal His-tag was expressed in Sf21 insect cells using the baculovirus expression system. The expression construct was obtained by PCR-amplification using the rAAV-expression construct as the template. Primers used for the amplification were: 5'-CGCGGATCCCGGTCCGAAGCGCGCGGAATTCAAAGGAGCTTTTCGCCACC ATGGAGACAGACACACTCCTGC-3' (forward) and 5'-CGCGGTACCTCAATGATGATGATGATGAAAATCTAAAGGTCTGAATCATCATAGT-3' (reverse). VA1 protein was expressed and purified as in ⁵.

For binding assays, VEGFR-2 domains 2+3 (R2D2-3; residues 118 to 326),⁷ VEGFR-1 domains 1-2 (R1D1-2, residues 23-224) and Tie2 ligand-binding domains (LBD, residues 1-444) were cloned into the pFastBac baculovirus expression vector with a C-terminal Fc-tag (human IgG1; VEGFR-1 and -2) or with a C-terminal Histidine-tag (Tie2). The constructs were expressed in Sf21 insect cells and purified by Protein A Sepharose or Ni²⁺-affinity step (GE Healthcare) followed by gel filtration on a Superdex 200 column in 10 mM HEPES, 0.1 M NaCl at pH 7.5. A Factor Xa cleavage site allowed the proteolytic Fc-tag removal and the preparation of the monomeric VEGFR-1 D1-2 construct.

Affinity measurements.

Isothermal calorimetric titrations of VA1 protein to soluble VEGFR-2 (D2-3, Fc-fusion), Tie2 (LBD, His-tagged) and VEGFR-1 (D1-2, monomeric) were carried out at 25°C using a VP-ITC calorimeter (MicroCal, GE Healthcare, Waukesha, WI). To control for heat dilution effects, all the protein buffers were adjusted to Hepes buffered sodium chloride at pH 7.5 by gel filtration. The receptor constructs were used in the calorimeter cell at a concentration of 5-8 μ M, and the VA1 ligand in the syringe at a concentration of about 0.10 mM. Data were processed using the MicroCal Origin 7.0 software.

VE-cadherin phosphorylation/internalization and Src phosphorylation assays.

To measure VE-cadherin tyrosine phosphorylation, HUVECs were grown to confluence, serum-starved and stimulated with the indicated proteins (500 ng/ml of each) for 5 min. The cells were then fixed and permeabilized with 3% paraformaldehyde (PFA), 0.5% Triton-X100 (Tx) in PBS for 3 min followed by further 15 min fixation with 3% PFA in PBS. Affinity purified rabbit antibody to VE-cadherin P-Tyr658 peptide was produced and purified by New England Peptide. Antibody (10 μ g/ml in PBS containing 1% BSA) was further purified by three absorption cycles on VE-cadherin null ECs (30 min VEGF stimulated, fixed, permeabilized and blocked with 5% BSA) for 1 h at room temperature (RT). Donkey antibodies to the appropriate species conjugated with Alexa-Fluor 555 (Molecular Probes, Invitrogen, Carlsbad, CA) were used as secondary antibodies. The primary and secondary antibodies were diluted in 5% BSA, 5% donkey serum in PBS. Epifluorescence microscope (Leica Microsystems GmbH, Wetzlar, Germany) images

Confidential manuscript

were captured using a CCD camera. Confocal microscopy was performed with a Leica TCS SP2 microscope with 40X oil immersion objective (Leica Microsystems). For quantification, the intensity of fluorescence signal for VE-cadherin P-Tyr658 was evaluated using ImageJ software (The National Institutes of Health, Bethesda, MD) after segmentation with the triangle algorithm.

VE-cadherin internalization assay was performed as previously described.⁶ Briefly, to measure internalization of endogenous VE-cadherin, HUVECs were treated with chloroquine 300 μ M for 3 h. Cells were incubated with mouse monoclonal BV-6 antibody (mAb) directed against the VE-cadherin extracellular domain (Millipore, Billerica, MA) for 1 h at 4°C in MCDB131 buffer, supplemented with 1% BSA medium. Cells were then rinsed with ice-cold MCDB131 to remove unbound antibody and treated with the indicated proteins (500 ng/ml of each) for 5 or 30 min. The cells were then lysed and surface VE-cadherin was immunoprecipitated, followed by western blotting for VE-cadherin with the same mouse monoclonal BV-6 antibody.

Src (Tyr416) phosphorylation was determined by western blotting in total cell lysates of HUVECs, cultured and stimulated as described above for VE-cadherin internalization studies, using rabbit monoclonal anti-phospho-Src (Tyr416) antibody (Cell Signaling Technology Inc., Danvers, MA). Total Src was determined using rabbit monoclonal anti-Src antibody (Cell Signaling Technology Inc.). In this experiment, HRP-generated chemiluminescence was acquired and recorded using the Chemidoc system (Bio-Rad).

MTT cell survival assay and analysis of protein expression by IP.

For analysis of protein expression, supernatants containing the growth factors of interest were produced by rAAV vector transfection of 293T cells using the jetPEI transfection reagent (Polyplus-transfection). Proteins were metabolically labeled with [³⁵S]Cys/Met (Amersham Biosciences and GE Healthcare), [³⁵S]-labelled growth factors were precipitated with VEGFR-1-Ig, VEGFR-2-Ig or VEGFR-3-Ig^{7,8} or Tie2-Ig (R&D Systems, Minneapolis, MN) and protein A sepharose, and analyzed with SDS-PAGE and autoradiography.

hVEGFR-1/EpoR-BaF3 and mVEGFR-2/EpoR-BaF3 cells are derived from the IL-3-dependent mouse pro-B cell line, BaF3.^{9,10} These cells undergo apoptosis in IL-3-deficient medium, but they can be rescued by the addition of the respective VEGFR ligands. hVEGFR-2/EpoR-BaF3 were made in a similar way (Dr Michael Jeltsch, University of Helsinki, PhD, unpublished data, 2011). For analysis of growth factor activity, 50 µl of serial dilutions of conditioned media (or purified proteins), as well as positive and negative controls, were applied to the wells of 96-well plates in triplicate. Subsequently, 20,000 VEGFR-1/EpoR-BaF3 cells in 50 µl were added to each well and the cells were incubated at 37°C for 48 h. MTT substrate was added, and the cells were incubated at 37°C for 2 h, lysis buffer (10% SDS, 10 mM HCl) was added, and the plates were incubated at 37°C overnight for color development. Quantification was done by absorbance at 540 nm. When the mammalian cell supernatants were used, the small values obtained with conditioned medium from untransfected cells were subtracted.

Immunocytochemistry.

HUVECs (PromoCell) overexpressing Tie2 fused in-frame to green fluorescent protein (HUVEC-Tie2-GFP) were made by transfection with a Tie2-GFP retrovirus, as described.¹¹ In an analogous way, BECs (PromoCell) overexpressing human VEGFR-2 fused in-frame to cyan fluorescent protein CFP (BEC-VEGFR-2-CFP) were made by transfection with a VEGFR-2-GFP retrovirus. The cells were cultured in complete endothelial cell growth medium MV (PromoCell) on coverslips. Stimulation with the indicated factors was done for 45 min. The samples were analyzed with a LSM 510 Meta confocal microscope equipped with digital camera (Carl Zeiss AG, Oberkochen, Germany; objectives 40x Plan-Neofluar 1.30, DIC or 63x Plan-Neofluar 1.25, DIC, Ph3; acquisition LSM software release 3.2).

Biotinylation experiments.

BECs were starved o/n in serum-free medium, stimulated with growth factors as indicated and treated with Sulfo-NHS-LC-Biotin (Thermo Fisher Scientific, Rockford, IL), as recommended by the manufacturer. After the treatment, the cells were lysed (1% Triton X-100 in PBS, supplemented with protease inhibitors), biotinylated proteins were precipitated by using the streptavidin-agarose resin (Thermo Fisher Scientific) and analyzed by SDS-PAGE and western-blotting with goat anti-human Tie1, Tie2 or VEGFR-2 antibodies (R&D Systems).

Ubiquitinylation experiments.

BECs were starved o/n in serum-free medium, stimulated as indicated and lysed (1% NP-40 in 40 mM Tris-HCl, pH7.4, 150 mM NaCl, supplemented with protease

inhibitors). VEGFR-2 or Tie2 were immunoprecipitated with polyclonal antibodies (R&D Systems). Precipitated proteins were run in SDS-PAGE and analyzed by Western blotting using mouse monoclonal antibodies against polyubiquitin-conjugated proteins (Enzo Life Sciences).

Cross-linking experiments.

BECs were starved for 3 h, treated with the indicated proteins for 20 min, and then with DTSSP (3,3'-Dithiobis(sulfosuccinimidyl propionate)) for 30 min. The cells were lysed, solubilized proteins were immunoprecipitated with anti-VEGFR-2 antibodies and Western-blotted with anti-Tie2.

Tissue transduction with the rAAV vectors.

For transduction of the ear skin, six to seven week-old female C57BL/6 mice were anesthetized with xylazine and ketamine and 5×10^9 rAAV particles (in 10 μ l volume) were injected into each ear. One week after the injections the mice were perfusion-fixed, and the ears were harvested, PFA-fixed and whole-mount stained.

Quantification of protein expression in transduced skeletal muscle.

rAAV-transduced muscles were weighed and homogenized in 0.2% Triton X-100 in PBS supplemented with protease inhibitors, using PowerLyzerTM 24 Bench Top Bead-Based Homogenizer (MO BIO Laboratories Inc., Carlsbad, CA). A ninety-six well maxisorp plate (Nunc, Thermo Fisher Scientific) was coated with 10 μ g/ml hVEGFR-1-Ig⁶ for VEGF or Tie2-Ig (R&D Systems) for VA1 in PBS, blocked with 5% BSA in TBST, after which the samples were applied and incubated for 2 h at RT. After extensive washing with TBST, the bound proteins (VEGF and VA1) were

Confidential manuscript

detected with goat anti-human VEGF antibody AF293 (R&D Systems), diluted in 2.5% BSA in TBST, followed by washing and incubation with rabbit anti-goat HRP conjugate (Dako, Glostrup, Denmark). Excess conjugate was washed away with TBST and the substrate SureBlue (KPL Inc, Gaithersburg, MD) was added for color development. The reaction was stopped by addition of an equal volume of 1M HCl, and OD at 450 nm was determined. The calibration curve was made with pure VA1 protein, made in S2 cells (see above), or VEGF (R&D Systems).

Whole-mount staining of mouse ears.

Separate ear leaflets, pinned to Sylgard plates were fixed with 4% PFA, washed with 0.3% Triton-X in PBS and blocked with donkey immunomix. Primary antibodies and secondary antibody-Alexa fluor conjugates (Molecular Probes, Invitrogen) were also diluted in donkey immunomix.

Acute skin permeability test.

FvB/N mice were anesthetized and injected i.v. with 300 μ l of 1% EvansBlue. Back skin on the back was shaved and 20 μ l of VEGF or VA1 in PBS (500 ng/ μ l) was injected into the dermis. After 1 hour, the mice were perfused with 10 ml of PBS via cardiac perfusion, skin pieces were excised, photographed and weighed. The dye was extracted overnight with deionized formamide (1 ml per a muscle) and measured at OD620 nm.

Doppler ultrasound measurement of blood perfusion.

Doppler ultrasound (VEVO 770 Micro-Ultrasound System, VisualSonics Inc., Toronto, Canada) was used to analyze blood perfusion in the transduced healthy *t.a.* muscles of anesthetized mice two weeks post-transduction. Image stacks were

generated by three-dimensional scanning, and percent vascularity in the muscle mid region was analyzed using the VEVO 700 analysis software (VisualSonics).

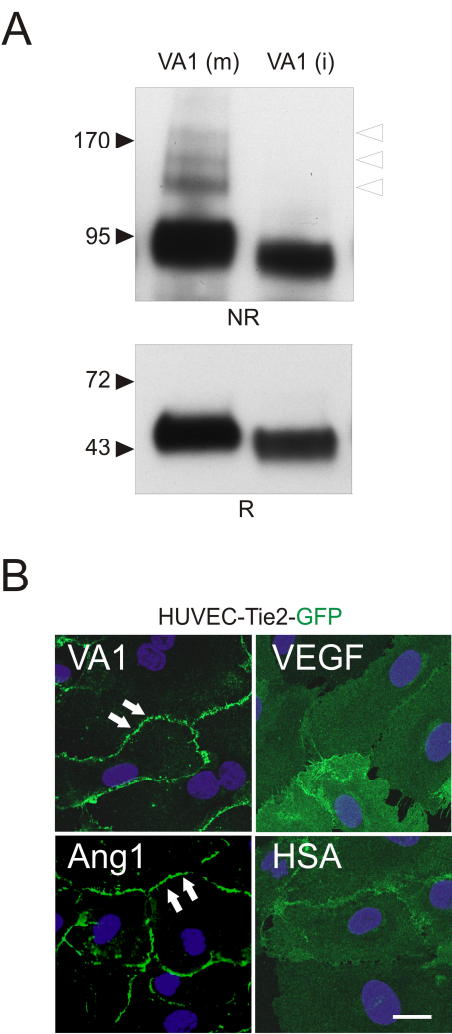
Mouse hindlimb ischemia model with rAAV delivery.

CAnN.Cg-Foxn1 nu/CrljOri nude male mice were obtained from Orient Bio, Korea. All mice were 6-12 weeks (16-24 g) of age at the time of study. Hind limb ischemia was induced by ligation and excision of the right femoral artery and vein under ketamine-xylazine anesthesia. For studies of the angiogenic potential, the mice were divided into 3 groups one day before the induction of ischemia. Mice (n=5 in each group) received intramuscular injection of rAAV-HSA (control), rAAV-VEGF or rAAV-VA1 (30 μ l of 4×10^8 vp/ μ l of each virus dose). For NIR fluorescence imaging, the previously described customized optical systems was used.¹³ Briefly, this system employs a CCD digital camera (PIXIS 1024; Princeton Instruments, Trenton, NJ) with a custom-made 830-nm band-pass filter (Asahi Spectra USA Inc., Torrance, CA) and 760-nm light-emitting diode arrays (SMC760; Marubeni America, New York, NY). For time-series ICG imaging, mice under ketamine-xylazine anesthesia were injected with an i.v. bolus of ICG (0.16 ml of 400 mM/l; Sigma-Aldrich) into the tail vein. ICG fluorescence images were obtained in a dark room for 6 minutes at 1-second intervals immediately after the injection. After acquiring the serial imaging, customized computer programs were used to obtain perfusion maps and necrosis ratio.

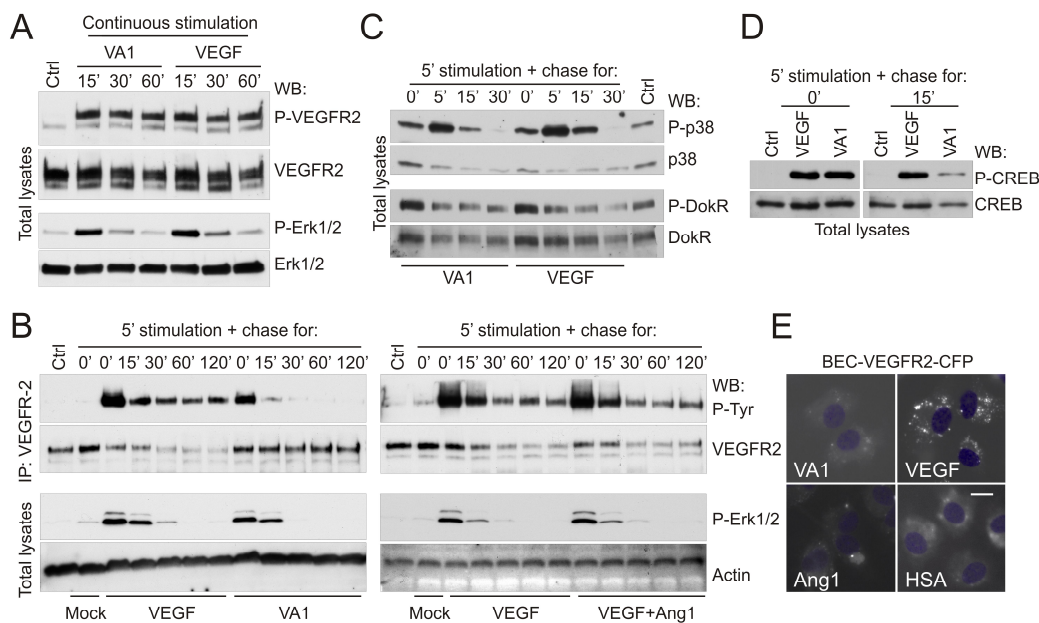
Mouse hindlimb ischemia model with protein delivery.

BALB/cAnNCrIjOri male mice were obtained from Orient Bio. The mice were 6–8 weeks (19–25 g) of age at the time of study. Murine hind limb ischemia was induced by ligation and excision of the right femoral artery and vein under ketamine-xylazine

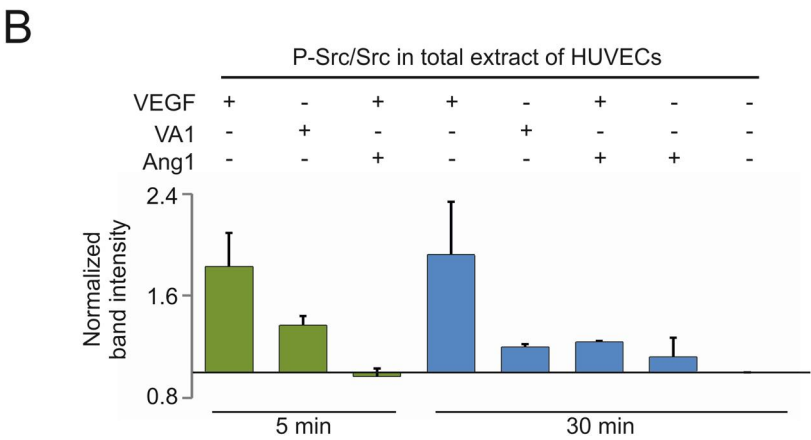
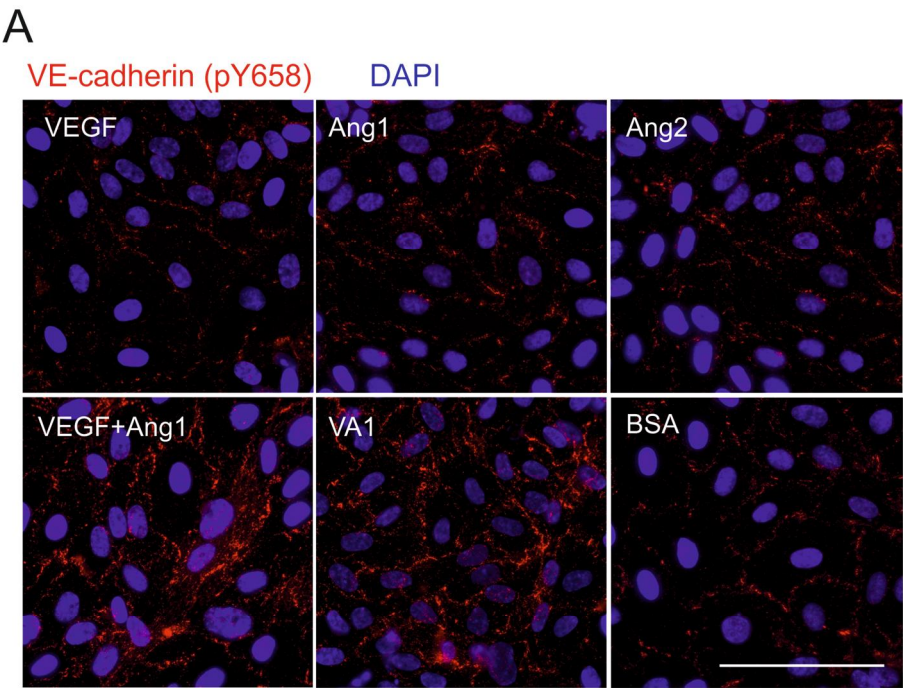
anesthesia. For therapeutic angiogenesis studies, the mice were divided into 3 groups after induction of ischemia. Mice (n=5 in each group) received intramuscular injection of BSA (20 μ l of 0.1% BSA) as a control, VEGF (20 μ l of 130 ng/ μ l), or VA1 (20 μ l of 260 ng/ μ l). A higher VA1 dose, compared to VEGF was used to equalize molar amounts of the proteins. Serial ICG perfusion imaging was performed immediately after surgery, and on post-operative days (POD) 3 and 7. NIR fluorescence imaging was performed as described above.



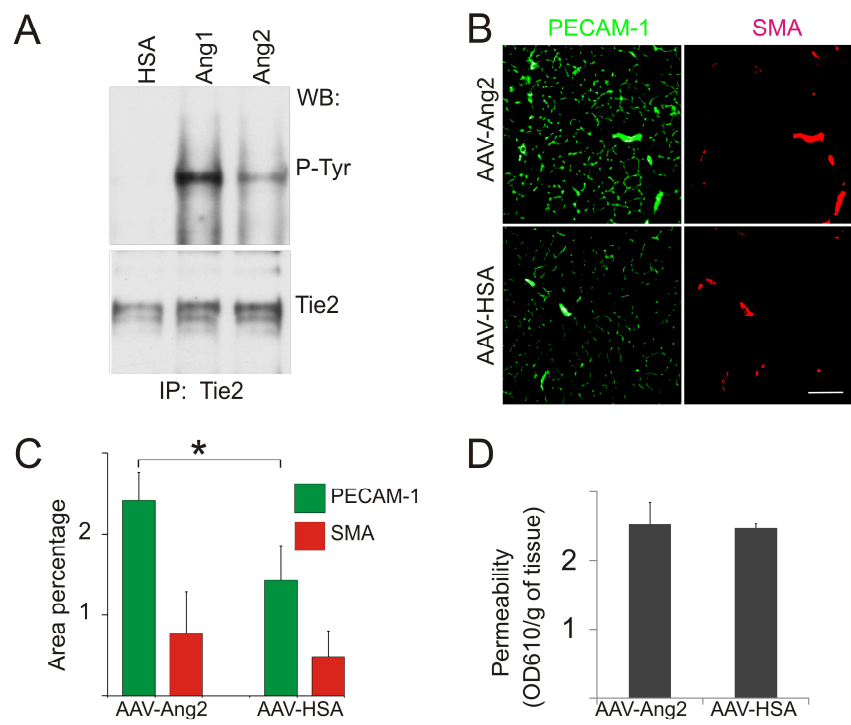
Anisimov et al., Figure S1



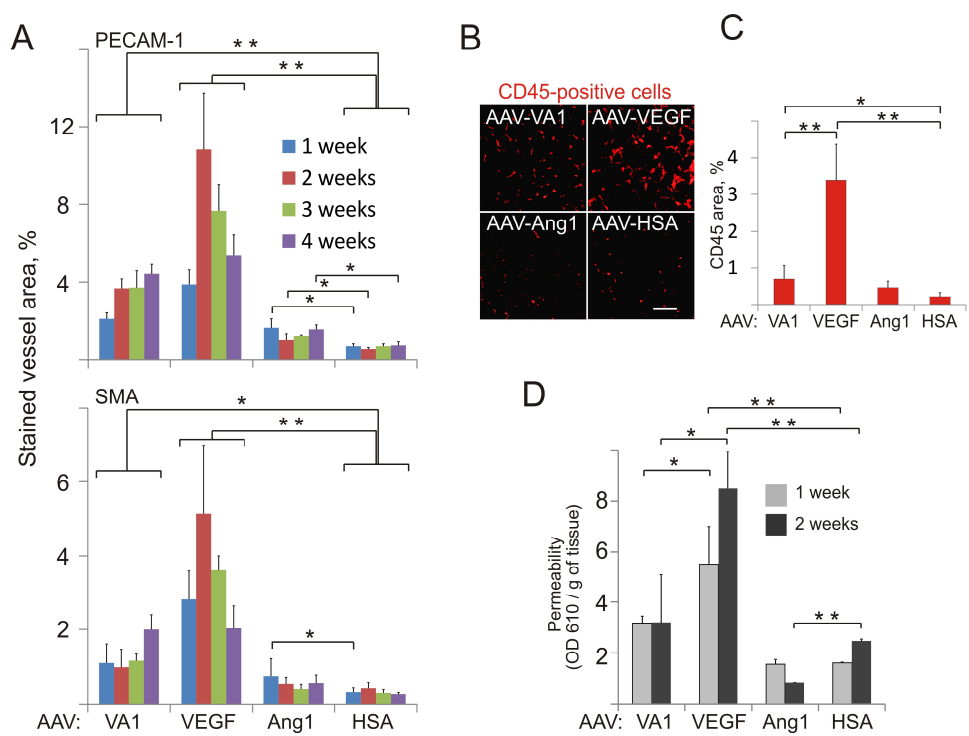
Anisimov et al., Figure S2



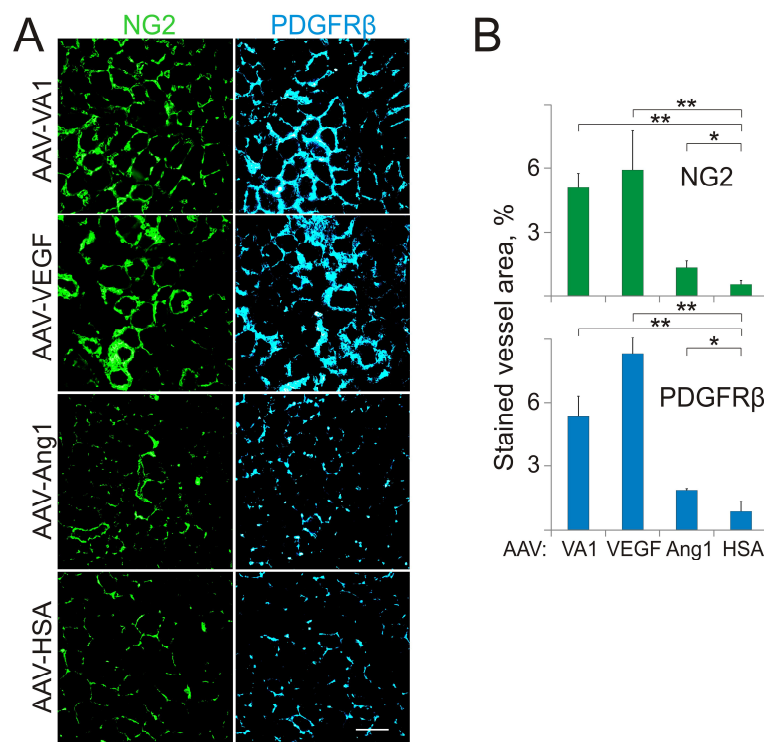
Anisimov et al., Figure S3



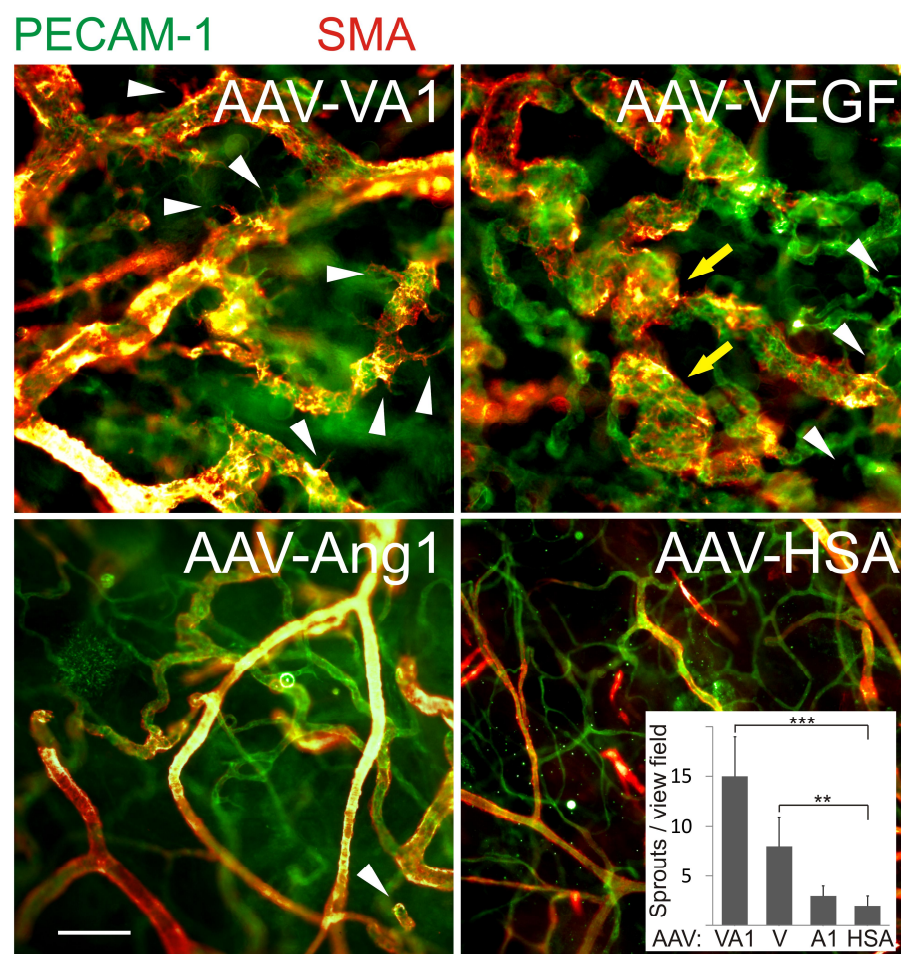
Anisimov et al., Figure S4



Anisimov et al., Figure S5



Anisimov et al., Figure S6



Anisimov et al., Figure S7

Supplemental figure legends

Figure S1. VA1 promotes Tie2 accumulation in cell-cell junctions. (A) VA1 proteins produced in 293T cells and Sf21 insect cells were analyzed by gel electrophoresis in non-reducing (NR) vs. reducing (R) conditions and western blotting with polyclonal antibody directed against VEGF. Note that VA1 produced in mammalian 293T cells reveals a small fraction of high-order multimers. (B) Fluorescent images of junctional Tie2 localization in HUVEC-Tie2-GFP cells treated with the mammalian cell-derived factors for 45 min. Representative images from three independent experiments are presented. Scale bar: 20 μ m.

Figure S2. Comparison of VA1 and VEGF-induced signal transduction and VEGFR-2 trafficking. (A) VEGFR-2 (Y1175) phosphorylation and total VEGFR-2 protein in BECs subjected to continuous stimulation with purified VA1 and VEGF for the indicated periods. Ctrl: control. Note that VA1 induces somewhat weaker Erk1/2 phosphorylation than VEGF. (B) 5 min stimulation of BECs was followed by incubation without ligands (chase) for the indicated time periods. Cells were lysed, VEGFR-2 was immunoprecipitated and P-Tyr was determined by western-blotting. In parallel, P-Erk1/2 was determined in the total lysates; (C) Comparison of VA1 and VEGF induced phosphorylation of MAP kinase p38 and DokR in BECs. (D) CREB phosphorylation at Ser133 in BECs stimulated with the indicated ligands. Note that the phosphorylation decays faster after with VA1 than with VEGF. (E) VA1 promotes less internalization of fluorescent VEGFR-2 than VEGF. Serum-starved BEC-VEGFR-2-CFP cells were stimulated with the indicated factors for 45 min, fixed and subjected to fluorescence microscopy. The nuclei were counterstained with DAPI. Scale bar: 20 μ m

Figure S3. VE-cadherin and Src phosphorylation in HUVEC cells after treatment with the indicated proteins. (A) VE-cadherin phosphorylation in HUVECs. The details of the experiment are described in the legend of **Fig. 3A** and in the Materials and methods. The panels are representative of two independent experiments. Scale bar: 100 μ m. (B) Cumulative quantification data of Src phosphorylation western blots, obtained from two independent experiments. The details are explained in Fig. 3C legend and in the materials and methods.

Figure S4. Analysis of Ang2 activity. (A) Phosphorylation of Tie2 was analyzed in HUVECs stimulated for 10 min with Ang1 or Ang2 (both at 250 ng/ml); (B) Comparison of PECAM-1 and SMA staining in *t.a.* muscles two weeks after transduction with rAAVs encoding Ang2 or HSA; (C) Quantification data from (B); (D) Blood vessel permeability measured by Miles assay in skeletal muscle treated in the same conditions as in (B). Data in A and D are representative of two independent experiments. Data in B are representative of three independent experiments. In (C) Students' unpaired *t*-test was used. Error bars: mean \pm SD. (*) – $p \leq 0.05$. Scale bar in B: 100 μ m.

Figure S5. Time-dependent vascular changes and inflammatory cell recruitment in *t.a.* mouse muscles transduced with the indicated rAAVs. (A) Quantification of total PECAM-1 and SMA positive vessel areas. Experimental conditions and asterixes are described in Figure 4 (A, B) legend. ANOVA, followed by Dunnett *post-hoc* test was used. (B) Representative images of anti-CD45 staining in sections from *t.a.* muscles of FVB/N female mice treated for two weeks with the indicated rAAVs.

Scale bar: 100 μm .; (C) Quantification of (B); (D) Miles permeability assay one and two weeks after transduction with rAAV at $1.34\text{E}+10$ vp in 30 μl per muscle. In (C) and (D) ANOVA, followed by Tukey *post-hoc* test was used.

Figure S6. VA1 and VEGF induce similar levels of pericyte coverage. *T.a.* muscles were injected with rAAVs encoding VA1, VEGF, Ang1 and HSA. After two weeks the muscles were dissected, sectioned and stained for the indicated antigens. Data in (A) are representative of three independent experiments. Representative images are shown. Scale bar: 100 μm . (B) Quantification data from (A). Error bars, mean \pm SD. ANOVA, followed by Dunnett *post-hoc* test was used. (*): $p \leq 0.05$, , (**): $p \leq 0.01$.

Figure S7. VA1 leads to vessel dilation and induces more sprouting than VEGF in the ear skin, but does not lead to development of glomeruloid angiomas. Ears of FVB/N female mice were injected with the indicated rAAVs ($8.0\text{E}+10$ vp/ear) and analysed by whole-mount staining for PECAM-1 and SMA one week thereafter. Representative images are shown. White arrowheads show sprouts, yellow arrows point to angiomas. The inset shows sprout quantification. Scale bar: 100 μm .

Supplemental references

1. Anisimov A, Alitalo A, Korpisalo P, Soronen J, Kaijalainen S, Leppanen VM, Jeltsch M, Yla-Herttuala S, Alitalo K. Activated forms of VEGF-C and VEGF-D provide improved vascular function in skeletal muscle. *Circ Res.* 2009;104:1302-1312.

2. Paterna JC, Moccetti T, Mura A, Feldon J, Bueler H. Influence of promoter and WHV post-transcriptional regulatory element on AAV-mediated transgene expression in the rat brain. *Gene Ther.* 2000;7:1304-1311.
3. Okabe M, Ikawa M, Kominami K, Nakanishi T, Nishimune Y. 'Green mice' as a source of ubiquitous green cells. *FEBS Lett.* 1997;407:313-319.
4. Cho CH, Kammerer RA, Lee HJ, Steinmetz MO, Ryu YS, Lee SH, Yasunaga K, Kim KT, Kim I, Choi HH, Kim W, Kim SH, Park SK, Lee GM, Koh GY. COMP-Ang1: a designed angiopoietin-1 variant with nonleaky angiogenic activity. *Proc Natl Acad Sci U S A.* 2004;101:5547-5552.
5. Leppanen VM, Jeltsch M, Anisimov A, Tvorogov D, Aho K, Kalkkinen N, Toivanen P, Yla-Herttuala S, Ballmer-Hofer K, Alitalo K. Structural determinants of vascular endothelial growth factor-D receptor binding and specificity. *Blood.* 2011;117:1507-1515.
6. Xiao K, Allison DF, Kottke MD, Summers S, Sorescu GP, Faundez V, Kowalczyk AP. Mechanisms of VE-cadherin processing and degradation in microvascular endothelial cells. *J Biol Chem.* 2003;278:19199-19208.
7. Makinen T, Jussila L, Veikkola T, Karpanen T, Kettunen MI, Pulkkanen KJ, Kauppinen R, Jackson DG, Kubo H, Nishikawa S, Yla-Herttuala S, Alitalo K. Inhibition of lymphangiogenesis with resulting lymphedema in transgenic mice expressing soluble VEGF receptor-3. *Nat Med.* 2001;7:199-205.
8. Leppanen VM, Prota AE, Jeltsch M, Anisimov A, Kalkkinen N, Strandin T, Lankinen H, Goldman A, Ballmer-Hofer K, Alitalo K. Structural determinants of growth factor binding and specificity by VEGF receptor 2. *Proc Natl Acad Sci U S A.* 2010;107:2425-2430.

9. Makinen T, Veikkola T, Mustjoki S, Karpanen T, Catimel B, Nice EC, Wise L, Mercer A, Kowalski H, Kerjaschki D, Stacker SA, Achen MG, Alitalo K. Isolated lymphatic endothelial cells transduce growth, survival and migratory signals via the VEGF-C/D receptor VEGFR-3. *EMBO J*. 2001;20:4762-4773.
10. Achen MG, Jeltsch M, Kukk E, Makinen T, Vitali A, Wilks AF, Alitalo K, Stacker SA. Vascular endothelial growth factor D (VEGF-D) is a ligand for the tyrosine kinases VEGF receptor 2 (Flk1) and VEGF receptor 3 (Flt4). *Proc Natl Acad Sci U S A*. 1998;95:548-553.
11. Saharinen P, Eklund L, Miettinen J, Wirkkala R, Anisimov A, Winderlich M, Nottebaum A, Vestweber D, Deutsch U, Koh GY, Olsen BR, Alitalo K. Angiopoietins assemble distinct Tie2 signalling complexes in endothelial cell-cell and cell-matrix contacts. *Nat Cell Biol*. 2008;10:527-537.
12. Li Y, Song Y, Zhao L, Gaidosh G, Laties AM, Wen R. Direct labeling and visualization of blood vessels with lipophilic carbocyanine dye DiI. *Nat Protoc*. 2008;3:1703-1708.
13. Kang Y, Choi M, Lee J, Koh GY, Kwon K, Choi C. Quantitative analysis of peripheral tissue perfusion using spatiotemporal molecular dynamics. *PLoS One*. 2009;4:e4275.